KINETIC STUDY OF THE HYDROGEN PEROXIDE OXIDATION OF CHROMIUM(III) TO CHROMIUM(VI)

by

MARTIN KNOBLOWITZ

A dissertation submitted to the Graduate Faculty in Chemistry in partial fulfillment of the requirements for the degree of Doctor of Philosophy, The City University of New York

1975

This manuscript has been read and accepted for the Graduate Faculty in Chemistry in satisfaction of the dissertation requirement for the degree of Doctor of Philosophy.

10/14/75
date

Jack S. Waugh
Chairman of Examining Committee

10/14/75
date

Leonard H. Schwartz
Executive Officer

Edwin H. Abbott

Michael W. Lerner
Supervisory Committee

The City University of New York

ABSTRACT

KINETIC STUDY OF THE HYDROGEN PEROXIDE
OXIDATION OF CHROMIUM(III) TO CHROMIUM(VI)

by

MARTIN KNOBLOWITZ

Adviser: Professor Jack I. Morrow

The kinetics of the oxidation of chromium(III) to chromium(VI) by hydrogen peroxide was studied by means of the stopped-flow technique. Complexities in the kinetic traces at 594 nm, where reactant absorbs, and at 374 nm, where product absorbs, raised the possibility of reaction intermediates. Construction of a time-spectrum established the presence of an intermediate, identified as a chromium(V) species through the use of esr spectroscopy, which could be most conveniently studied at 500 nm.

The processes visible at 500 nm were that of the formation and loss of an intermediate. The rate of the formation step was dependent on the hydrogen peroxide concentration and inversely dependent on the hydroxide concentration. The rate of loss was independent of both these reagents. At fixed chromium concentration, the magnitude of the absorbance change was found to be dependent on the hydrogen peroxide concentration and inversely dependent on the hydroxide concentration. The possibility

of an equilibrium as the explanation for this last observation was rejected for three reasons: 1) The magnitude of the absorbance change at 594 nm was not affected by variation in the hydrogen peroxide and hydroxide concentrations. 2) Use of a chelating agent significantly reduced the absorbance change at 500 nm with only minor effect at 594 nm. 3) The esr spectra show that no chromium(III) remains when the chromium(V) species is being monitored.

A branching mechanism, with chromium(IV) and chromium(V) species produced along parallel paths, is proposed as the explanation of the preceding observations. A detailed mathematical treatment of this mechanism, including computer simulations, is presented. The overall reaction can be represented schematically by the sequence

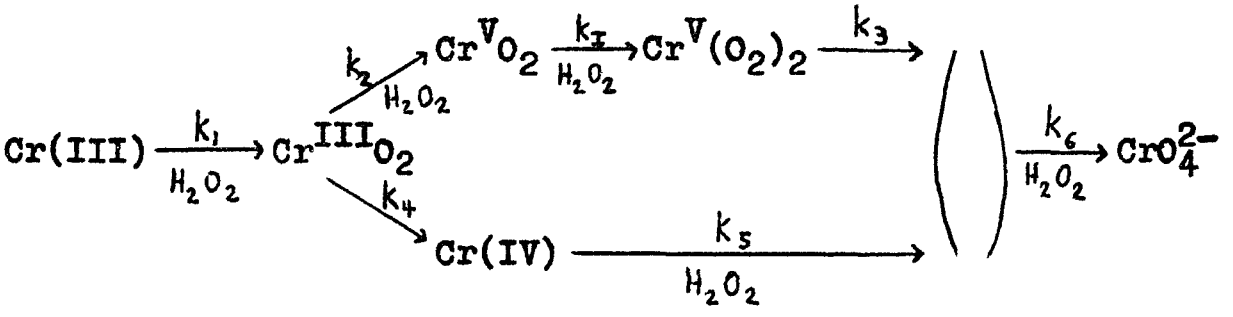

where the parentheses represent an intermediate(s) which could not be monitored. The values for the rate constants are: $k_1 = 5.3 \pm 1.0 \times 10^3\ M^{-1}\ sec^{-1}$, $k_2 = 2.0 \times 10^4\ M^{-1}\ sec^{-1}$ $k_3 = 0.11 \pm 0.02\ sec^{-1}$, $k_4 = 1.1 \times 10^2\ sec^{-1}$, $k_5 = 2.1 \pm 0.3 \times 10^2\ M^{-1}\ sec^{-1}$, $k_6 = 23 \pm 4\ M^{-1}\ sec^{-1}$. The values of k_2 and k_4 were not experimentally accessible but were calculated. The value of k_I cannot be determined.

TO MY PARENTS

BERNARD AND ESTHER

KNOBLOWITZ

ACKNOWLEDGMENT

I wish to express my most profound gratitude to Prof. Jack I. Morrow who has served as guide and inspiration. His unstinting assistance and incisive criticism has made this work possible. I am forever indebted to him.

TABLE OF CONTENTS

LIST OF TABLES

LIST OF FIGURES

Introduction

Oxidation-reduction reactions utilizing chromium in its various oxidation states have long been the subject of mechanistic studies.[1,2,3] Many investigations involved chromium(VI) due to its extensive use for preparative purposes. It is often used in aqueous or acetic acid media to oxidize primary alcohols or aldehydes to carboxylic acids and to oxidize secondary alcohols to ketones. The reasons for the continuing interest in reactions involving the reduction of chromium(VI) to chromium(III) are: the availability of a substantial body of information on the nature and stability of chromium(VI), the simplicity of product separation and identification due to the kinetic inertness of chromium(III) and, most important of all, the essence of the net process in these systems - chromium(VI) is undergoing a three-equivalent change while the reducing agent is generally undergoing a one- or two-equivalent change. In the absence of a one-step, three-electron transfer, there must be a sequence of steps involving intermediate oxidation states of chromium. With but a single exception,[4] studies have shown that such is indeed the case. The consequence is that reaction rates often follow complicated kinetic expressions. There is compensation, however, in that a more detailed formulation of the individual steps which comprise the net process is possible.

The earliest evidence for the existence of intermediate oxidation states of chromium was provided by the phenomenon

of induced oxidation. Two examples are the ferrous ion induced oxidation of iodide to iodine by chromic acid[5] and the arsenite induced oxidation of manganic salts by chromic acid.[6] In the former case, it is found that in dilute acid (0.001 N) reactions (1) and (2)

$$2\ HCrO_4^- + 6\ I^- + 14\ H^+ \longrightarrow 2\ Cr^{3+} + 3\ I_2 + 8\ H_2O \qquad (1)$$

$$2\ Fe^{3+} + 2\ I^- \longrightarrow 2\ Fe^{2+} + I_2 \qquad (2)$$

are very slow. Under the same conditions, reaction (3)

$$HCrO_4^- + 3\ Fe^{2+} + 7\ H^+ \longrightarrow Cr^{3+} + 3\ Fe^{3+} + 4\ H_2O \qquad (3)$$

is very rapid. When a solution of dilute acid, chromic acid, and iodide is treated with a ferrous salt solution, however, iodine is quickly liberated. Since I^- is not oxidized rapidly by $HCrO_4^-$ or by Fe^{3+} alone, an oxidizing agent more powerful than $HCrO_4^-$ must be formed. To determine the nature of this agent, the concept of an "induction factor" was created. The induction factor is the ratio of the equivalents of the reducing agent oxidized to the equivalents of the inductor oxidized. In practice, since both reducing agent and inductor compete for the chromium intermediate, the induction factor represents the theoretical limit approached when the reducing agent is in great excess over the inductor. In the reaction

$$HCrO_4^- + Fe^{2+} + 2\ I^- + 7\ H^+ \longrightarrow Cr^{3+} + Fe^{3+} + I_2 + 4\ H_2O \qquad (4)$$

the induction factor is two since I^- transfers two equivalents to every one transferred by Fe^{2+}. Thus the intermediate must be chromium(V).

The balanced equation for the arsenite induced oxidation of manganic salt by chromic acid is

$$2\ HCrO_4^- + 2\ H_3AsO_3 + Mn^{2+} + 6\ H^+ \longrightarrow 2\ Cr^{3+} + 2\ H_3AsO_4 + MnO_2 + 4\ H_2O \quad . \quad (5)$$

Here the induction factor is 0.5 and a chromium(IV) intermediate is indicated.

In more recent studies, the presence of chromium intermediates has been invoked to explain kinetic results and the findings of product analysis. In the study by Altman and King[7] of the rate of exchange of chromium(III) and chromium(VI), the rate expression was found to be

$$\text{Rate} = k_{ex}\left[Cr(H_2O)_6^{3+}\right]^{4/3}\left[HCrO_4^-\right]^{2/3} \quad . \quad (6)$$

The reaction order ($4/3 + 2/3 = 2$) suggested two chromium atoms in the transition state with an average oxidation number of four $\left[4/3(+3) + 2/3(+6) = 2(+4)\right]$. A mechanism consistent with these findings is

$$^*Cr^{3+} + Cr^{6+} \rightleftharpoons {}^*Cr^{4+} + Cr^{5+} \quad (7)$$

$$^*Cr^{3+} + Cr^{5+} \rightleftharpoons {}^*Cr^{5+} + Cr^{3+} \quad (8)$$

or

$$^*Cr^{3+} + Cr^{5+} \rightleftharpoons {}^*Cr^{4+} + Cr^{4+} \quad (9)$$

rate-determining step (rds)

$$^{*}Cr^{5+} + Cr^{6+} \rightleftharpoons {}^{*}Cr^{6+} + Cr^{5+} \qquad (10)$$

A study by Ardon and Plane[8] and its amplification by Hegedus and Haim[9] illustrate the power of product analysis as a method for gaining insight into reaction mechanisms. Ardon and Plane examined the products of the reduction of chromium(VI) by chromium(II) and found that 50% of the chromium taking part in the net reaction appeared in the form of a binuclear species which they assumed to have the form $Cr_2(OH)_2^{4+}$ (later confirmed by Kolaczkowski and Plane[10] through O^{18} exchange studies). The following sequence was proposed to explain the stoichiometry:

$$Cr(VI) + Cr(II) \longrightarrow Cr(V) + Cr(III) \qquad (11)$$

$$Cr(V) + Cr(II) \longrightarrow Cr(IV) + Cr(III) \qquad (12)$$

$$Cr(IV) + Cr(II) \longrightarrow Cr(OH)_2Cr^{4+} \qquad (13)$$

Hegedus and Haim tested the proposed mechanism by labelling the chromium(VI) and examining the distribution of labelled chromium in the products. The above mechanism was confirmed as the major pathway, but the discovery of a small but significant proportion of labelled chromium(III) product necessitated the modification of equation (12) to

$$^{*}Cr(V) + Cr(II) \xrightarrow{\sim 80\%} {}^{*}Cr(IV) + Cr^{3+} \qquad (14)$$

$$^{*}Cr(V) + Cr(II) \xrightarrow{\sim 20\%} {}^{*}Cr^{3+} + Cr(IV) \quad . \qquad (15)$$

Mention has been made of the fact that the chromium(III) products of chromic acid reactions are substitution inert. Reactions in which chromium(III) is oxidized to chromic acid should be instructive as the mechanisms may involve the same steps. In acidic media, chromium(III) can be oxidized only by relatively powerful oxidizing agents. Tong and King[11] studied the cerium(IV) oxidation of chromium(III) in acid. The rate law was found to be

$$d[Cr^{6+}]/dt = k[Ce^{4+}]^2\ [Cr^{3+}]/[Ce^{3+}] \quad . \tag{16}$$

The transition state has one cerium atom and one chromium atom ($2\ Ce^{4+} + Cr^{3+} - Ce^{3+}$) with an average oxidation state of +4 for each metal. On this basis, the following mechanism was proposed:

$$Ce^{4+} + Cr^{3+} \underset{k_2}{\overset{k_1}{\rightleftharpoons}} Ce^{3+} + Cr^{4+} \tag{17}$$

$$Ce^{4+} + Cr^{4+} \xrightarrow[k_4]{k_3} Ce^{3+} + Cr^{5+} \quad \text{(rds)} \tag{18}$$

$$Ce^{4+} + Cr^{5+} \underset{k_6}{\overset{k_5}{\rightleftharpoons}} Ce^{3+} + Cr^{6+} \tag{19}$$

From the first step, the equilibrium concentration of chromium(IV) is $[Cr^{4+}] = k_1[Cr^{3+}]\ [Ce^{4+}]/k_2[Ce^{3+}]$. The observed rate law indicates that $k_5[Ce^{4+}] \gg k_4[Ce^{3+}]$ and that the chromium(IV) to chromium(V) transition is the rate-controlling process. This oxidation sequence follows the general pattern for the reduction processes previously discussed.

A basic medium would facilitate the study of the

oxidation of chromium(III) to chromium(VI) because under such conditions the chromium(III) becomes more labile while the product, chromate, is kinetically inert. Enhanced reactivity of the hydroxo form of a metal ion is quite common in substitution and oxidation-reduction reactions.[12,13] A difficulty arises, however, in working with such a system. Any study involving transition metal ions must deal with the phenomenon of inorganic polymerization. The immediate problem raised by inorganic polymerization in any kinetic study is the ambiguity in the identity of the reactive species. In the case of a basic solution of chromium(III), there is an appreciable distribution of metal ion in various monomeric and polymeric forms. Since the degree of polymerization is a function of aging, with equilibrium approached only slowly (sometimes on the order of years[14]), the history of each solution becomes important.

One manifestation of increasing polymerization is the observation of a spectral shift when bridging occurs through oxo or hydroxo groups. Solutions containing monomeric chromium(III) are reddish-blue in color. Appreciable polymerization turns these solutions green. A method has been developed by Morrow and Levy[15] for the determination of the degree of polymerization from the extent of the spectral shift and applied to the chromium(III) system. A detailed discussion of inorganic polymerization in general is contained in a series of articles by Sillen[16] and by Pokras.[17]

Various studies have focused specific attention on polymerization in chromium systems. The phenomenon has been found to occur even at fairly low pH. As a case in point, Hall and Eyring[18] found that the acidity of chromic nitrate solutions increased upon aging. Typically, a 0.1 M $Cr(H_2O)_6(NO_3)_3$ solution prepared at pH = 2.60 and left to stand at room temperature for 26 days had a final pH = 2.37. They attributed this pH change to the formation of oxygen bridges between chromium ions.

In contrast, a study by Bjerrum and coworkers on the hydrolysis of chromium(III) in perchloric acid found it to be negligible. Solutions which were 0.02 M Cr^{3+} and 0.02 M $HClO_4$ were heated at 75° for 24 hours. The pH went from 1.70 to 1.69, which was within the experimental error. Heating to 75° for three more days had very little effect on acidity.

Postmus and King[14] had various concentrations of $Cr(H_2O)_6^{3+}$ (10^{-3} M to 5×10^{-2} M) in 0.0132 M $HClO_4$ heated to 74° for 50 hours. Measurements taken 1 to 10 hours after cooling indicated that the absorbancy index of Cr^{3+} had increased by 4 to 12%. In 1.0 M $HClO_4$, a solution 5×10^{-2} M in Cr^{3+} showed no change in absorbancy index after similar treatment. A value for the dissociation constant for the equilibrium expression

$$K = [H^+]\,[Cr(OH_2)_5OH^{2+}]/[Cr(OH_2)_6^{3+}] \qquad (20)$$

was determined. The value, $K = 1.5 \times 10^{-4}$, compared favor-

ably with previous values in the literature.

Laswick and Plane[20] studied the slow changes which take place when basic chromium solutions are refluxed. Following refluxing, the solutions were passed through ion exchange columns, the fractions eluted were oxidized to chromate by hydrogen peroxide and the amount of chromium in each sample was determined by spectrophotometric analysis. After 10 minutes of refluxing, a basic chromium solution was analyzed and found to consist of 85.7% monomer, 10.1% dimer, with the rest as a higher polymer and "residue". A reflux of 27 days duration produced a solution with the composition 76.2% monomer, 9.3% dimer, and the rest as a higher polymer and "residue".

In addition to determining the distribution of the various species, Laswick and Plane studied the spectra of each eluted fraction. The monomer was found to have absorbance maxima at 408 and 574 nm, with absorptivities of 15.6 and 13.4, respectively. The dimer had absorbance maxima at 418 and 582 nm with absorptivities of 22.5 and 16.9, respectively.

In order to obtain information on oxidation mechanisms in highly basic media, Baloga and Earley[21] investigated the oxidation of chromium(III) to chromium(VI) by hydrogen peroxide. They found it necessary to age their chromium solutions in base for fixed periods of time before adding alkaline hydrogen peroxide so as to insure a constant distribution of the various chromium species. Reaction orders were

determined by measuring initial rates. The effect of the degree of polymerization on rates of reaction was determined by varying the aging times of the chromium solutions, but no detailed mechanism was presented since the actual distribution of polymeric species was not known.

The chromium-hydrogen peroxide system in general is little understood. Several studies of peroxide complexes of intermediate oxidation states of chromium have been done. Garner and coworkers have succeeded in preparing a number of chromium(IV) diperoxo amines.[22,23] The synthesis of various peroxychromic species by the dropwise addition of hydrogen peroxide to chromic acid solutions at -9° to -4° is detailed in a paper by King and coworkers.[24] The species $Cr_2^{III}O_2^{4+}$ and $Cr_3^{III}(O_2)_2^{5+}$ were isolated.

Evans[25] investigated the nature of the peroxychromate species. As CrO_5 quickly decomposes in aqueous solution, the study was carried out in aqueous methanol. He found that the species CrO_5 obeyed Beer's law over a wide concentration range and, using Job's method, determined that CrO_5 has two peroxo groups. The kinetics of the formation of CrO_5 in nonaqueous media was investigated by Tuck and Walters[26] and by Wilkins and coworkers.[27] The reaction was found to be first order in both chromium(VI) and hydrogen peroxide.

Ardon and Plane[8] found that the reaction of chromium(II) with hydrogen peroxide in acid media produced monomeric chromium(III) and a dimeric species of chromium(III) which

was 14% of the total chromium. They speculated that this was due to the oxidation of chromium(II) by two pathways:

$$Cr^{2+} \longrightarrow Cr^{3+} \quad \text{1 electron path (monomeric)} \qquad (21a)$$

$$Cr^{2+} \longrightarrow Cr^{4+} \quad \text{2 electron path} \qquad (21b)$$

$$Cr^{2+} + Cr^{4+} \longrightarrow \text{dimeric species} \qquad (22)$$

The coordination numbers associated with the various oxidation states of chromium play an important role in the mechanisms of the electron transfer reactions in which chromium participates. Chromium(VI) is known to be four-coordinate.[28] Hunt and Taube[29] have established chromium(III) as six-coordinate through the use of isotopic exchange. It follows that the change from the +3 to the +6 state must be accompanied by a change in coordination number.

To establish at what point this coordination change takes place, it is necessary to examine the properties of chromium(IV) and chromium(V). Compounds of chromium(IV) and chromium(V) are relatively rare because of their sensitivity to air and moisture. It was found that K_2CrF_6 has the same x-ray diffraction pattern as K_2MnF_6, in which it is known that Mn(IV) has six fluoride ions surrounding it in an octahedral arrangement.[30,31] The chromium(V) compound $Ba_3(CrO_4)_2$ is isomorphous with $Ba_3(PO_4)_2$ which contains a tetrahedral anion.[32,33]

By analogy, chromium(IV) should have the same coordination as vanadium(III), with which it is isoelectronic.

Comparison of the visible spectra of ammonium vanadium alum (containing $V(H_2O)_6^{3+}$ ion) and vanadium(III) in solution[34] suggests a coordination number of six for vanadium(III). Chromium(V) and chromium(VI) are isoelectronic with Mn(VI) and Mn(VII), respectively, which have tetrahedral coordination with oxygen atoms in manganate and permanganate ions.[35,36] For these reasons, chromium(IV) and chromium(V) are considered to be six- and four-coordinate, respectively.

The coordination change in the transition from the +5 to the +4 state was the explanation proposed by Altman and King for the slowness (on the order of days) of the rate of exchange between chromium(III) and chromium(VI). Exchange between chromium(V) and chromium(VI) is expected to be rapid by analogy with the exchange between manganate and permanganate.[35,36] In similar fashion, the equilibrium

$$\overset{*}{\mathrm{Cr}}(\mathrm{III}) + \mathrm{Cr}(\mathrm{VI}) \rightleftharpoons \overset{*}{\mathrm{Cr}}(\mathrm{IV}) + \mathrm{Cr}(\mathrm{V}) \qquad (23)$$

is expected to be rapid by analogy with plutonium and neptunium systems.[37,38] From the above it can be seen that while the point at which the coordination change takes place is known, nothing is known about the process by which this change occurs.

With all its complexities - intermediates, possible parallel reaction pathways, change in coordination number - the chromium(III)-hydrogen peroxide reaction is a promising system for kinetic study. Although the mechanisms should be analogous, much more work has been done on the role of

chromium(VI) as an oxidizing agent than on the part played by chromium(III) as a reducing agent. It is the aim of the present work to provide additional insight into the role of chromium intermediates in redox reactions; in particular in the oxidation of chromium(III) to chromium(VI) by hydrogen peroxide in basic media.

Experimental Section

Materials. Stock solutions of $Cr(H_2O)_6^{3+}$ were prepared by the hydrogen peroxide reduction of sodium chromate (Baker Chemical Co.) in perchloric acid and the concentrations determined spectrophotometrically using a Beckman DU Spectrophotometer at 408 nm (ϵ=15.6) and at 574 nm (ϵ=13.4), the positions of maximum absorbance of the monomer.[20]

Hydrogen peroxide solutions of the desired concentrations were prepared from commercially available 30% H_2O_2 solution (Fisher Chemical Co.) without added stabilizers. The hydrogen peroxide was standardized by titration with potassium permanganate.

Carbonate-free sodium hydroxide stock solutions were standardized using potassium hydrogen phthalate. Periodically, the carbonate concentration was determined by titration of sodium hydroxide with hydrochloric acid to a phenolphthalein endpoint followed by titration to a methyl orange endpoint.[39] The levels of carbonate found to be present were such as to have a negligible effect on the kinetics of the reaction. In a kinetic run where an appreciable amount of carbonate was added, no catalytic effect was observed and the carbonate functioned solely as a base.

Spectral Study. A Cary Model 14 Recording Spectrophotometer was used to obtain the spectra of all solutions. The spectrum of the $Cr(H_2O)_6^{3+}$ stock solution is shown in Fig. (1a). Basic, metastable chromium(III) monomer (CrO_2^-), the spectrum

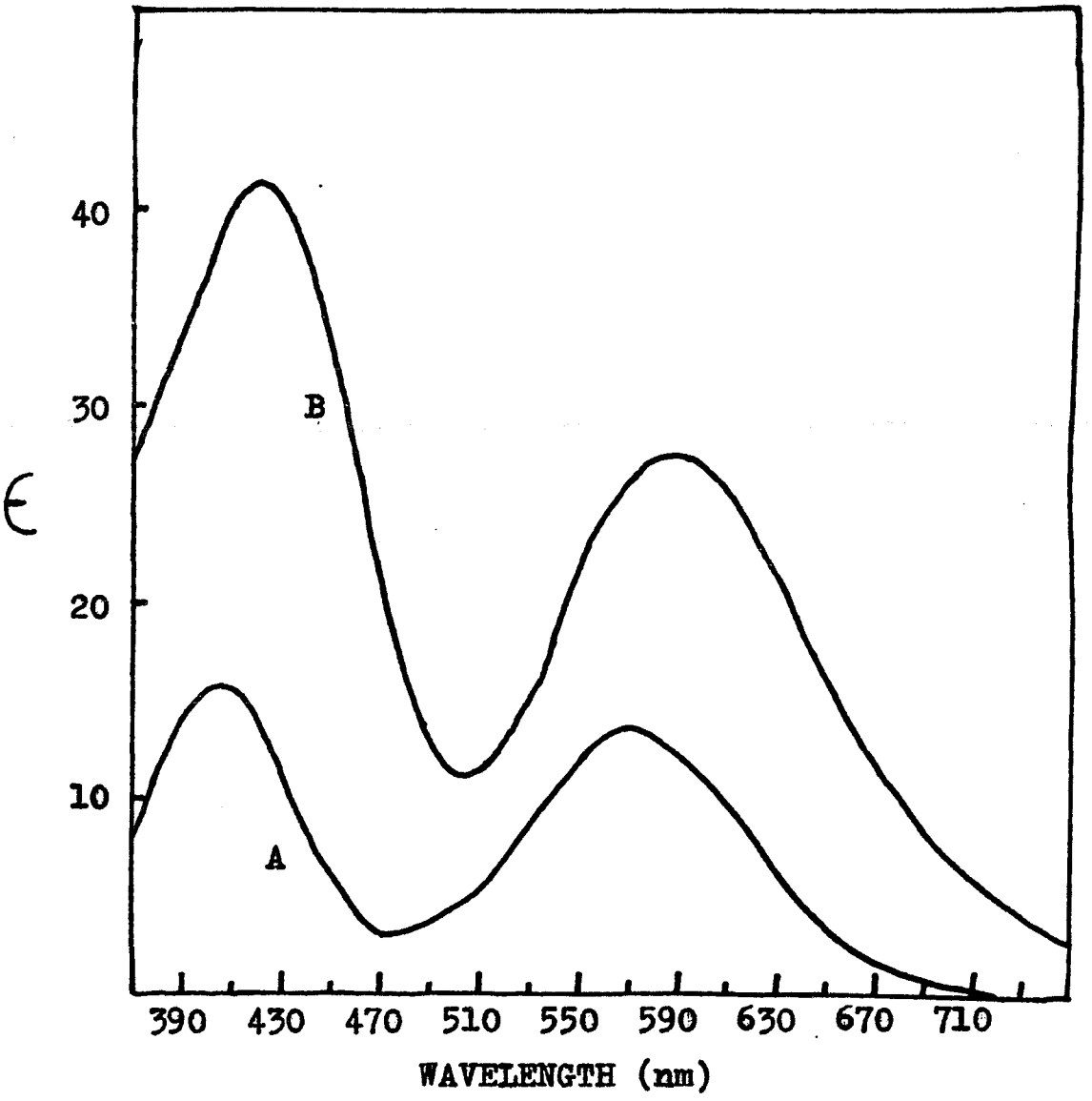

Figure 1. Absorption Spectra of Chromium(III):

A - in acid B - in base

of which is shown in Fig. (1b), has absorbance maxima at 425 and 594 nm (ϵ=27.1). The absorbance maximum of chromate is at 374 nm.[21]

Kinetic Measurements. In this study, the principal experimental method used is the stopped-flow technique. The Aminco-Morrow Stopped-Flow Apparatus (SFA)[40,41] shown schematically in Fig. (2), allows reactions with half-lives of milliseconds or longer to be followed spectrophotometrically. Fig. (3) shows the SFA in relation to the entire experimental system.

Two solutions, whose mixture will initiate the reaction, are stored in driving syringes. All components in the SFA which come in contact with reaction solutions - syringes, valves, connecting tubing, mixing chamber, and observation cell - are made from chemically resistant materials: Kel-F, teflon, ethylene-propylene rubber, glass, and quartz. Thermostating of solutions is achieved by the circulation of water through holes drilled into the aluminum block in which the driving syringes are mounted.

Upon simultaneous advancement of the pistons by compressed nitrogen, the two solutions are forced through teflon tubes into a teflon mixing chamber. From there they enter a quartz window observation cell with a path length of 10 mm. The dead time, the time required for the solution to reach the point of observation from the point of mixing, is 2 milliseconds for an observation cell with a 10 mm

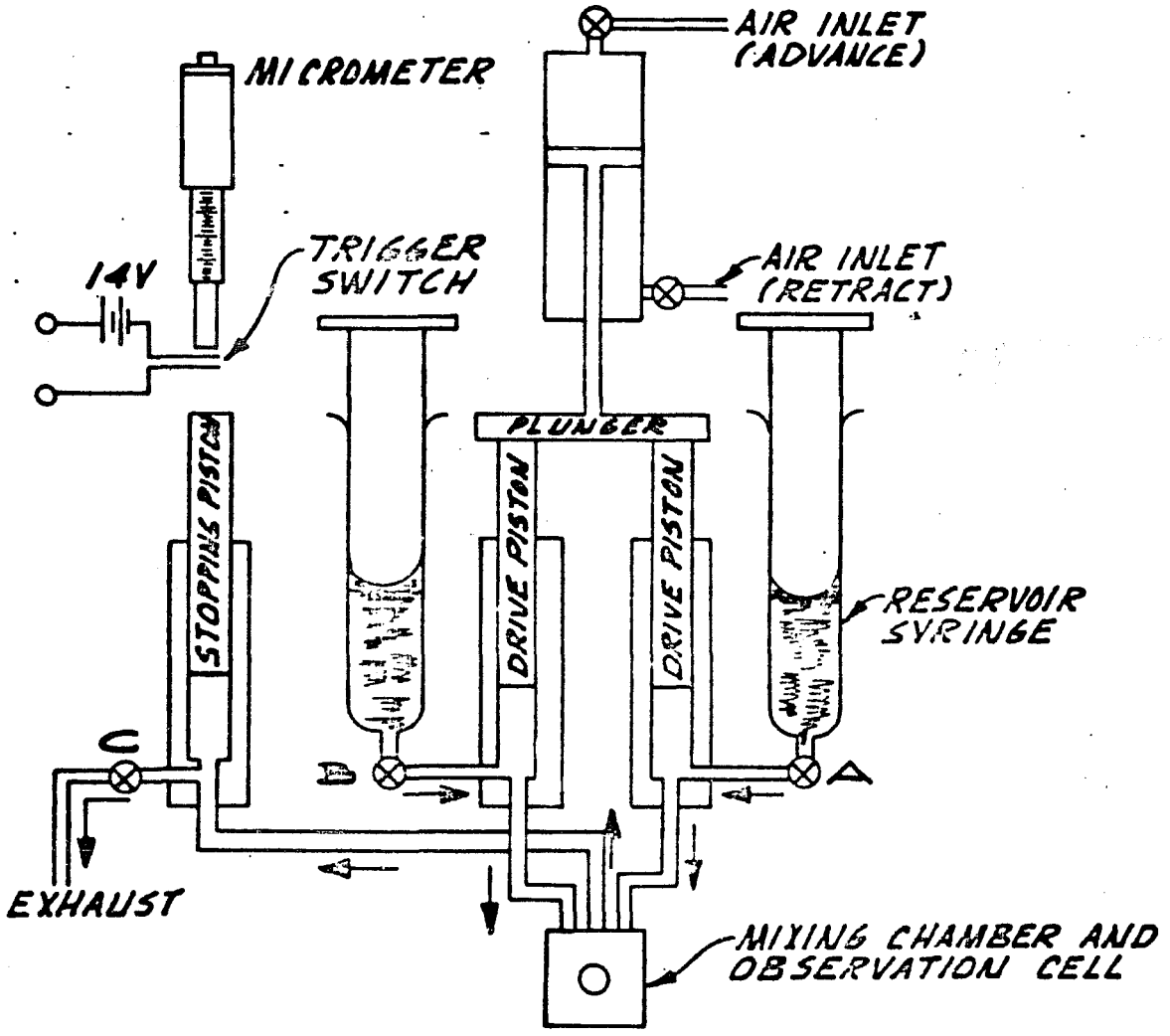

Figure 2. Schematic Diagram of an Aminco-Morrow Stopped-Flow Apparatus.

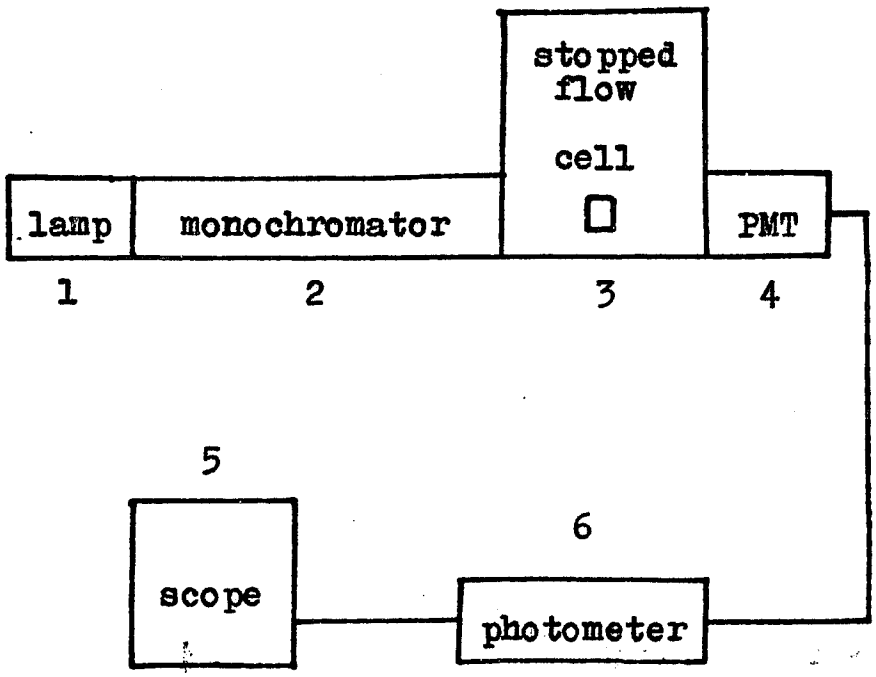

1 - The light source is a tungsten lamp powered by a Harrison 6274A dc power supply.
2 - The monochromator is a modified Beckman DU.
3 - The mixing system is an Aminco-Morrow Stopped-Flow Apparatus. The dead time is 2 msec. and the mixing time is less than 1 msec. with better than 98% efficiency.
4 - The detector is an R136 Photomultiplier Tube powered by a Harrison 6515A dc power supply.
5 - An Aminco Linear-Log Photometer permits offsetting, change of bandwidth, and selection of output as % transmittance or as absorbance.
6 - The change in absorbance is displayed as a trace on a Tektronix R564B Storage Oscilloscope.

Figure 3. Schematic Diagram of the Experimental System.

path length and a flow velocity of 14 ml/sec. The efficiency of mixing is greater than 98% in less than 1 millisecond after mixing begins.

After leaving the observation cell, the reaction mixture enters an exhaust chamber and advances the piston of a stopping syringe. When this piston contacts the tip of a micrometer, a switch is closed, triggering the storage oscilloscope. Typically, about 0.1 ml of each solution is used for each run, sufficient to flush any solution from previous runs and leave fresh solution in the observation cell. The transport time, the interval during which reactants flow, is on average about 10 milliseconds for the volumes of solution used.

Referring once again to Fig. (3), light from a tungsten source powered by a Harrison 6274A dc power supply passes through an Aminco Minimonochromator and then through the observation cell. Transmitted light is detected by an R-136 Photomultiplier Tube (PMT) powered by a Harrison 6515A dc power supply and the PMT output is fed into an Aminco Linear-Log Photometer where the signal is filtered and converted to a logarithmic (absorbance) signal which is displayed on a Tektronix R564B Storage Oscilloscope. A Polaroid camera is used to photograph the kinetic trace for later analysis.

In all kinetic runs, pseudo-order conditions [Appendix (I-A)] have been established. Of the two solutions in the driving syringes, one consisted of $Cr(H_2O)_6^{3+}$ and hydrogen

peroxide diluted to the desired concentrations from their respective stock solutions. The pH of this solution was approximately three. The second solution consisted of sodium hydroxide stock solution diluted to the desired concentration. Ionic strength was adjusted using sodium perchlorate. This experimental method insured that chromium(III) monomer was the species being oxidized because no base was added before initiation of the reaction. Rates of reaction were followed by measuring absorbance changes at 374, 500, and 594 nm. All solutions were thermostated at $25.0 \pm 0.1^{\circ}$ prior to initiation of reactions. There was a small temperature rise of less than one degree upon mixing of solutions.

Gas Evolution. Oxygen evolution during the course of the reaction was monitored by means of a gas buret.

ESR Study. Paramagnetic species generated during the reactions were detected and monitored with time using a JEOL LTD. JES-SM-1 continuous flow system in conjunction with a JES 3X JEOL esr spectrometer. To determine g values the field was calibrated using α,α'-diphenyl-β-picrylhydrazyl (DPPH) and the reaction monitored without resetting the klystron frequency.

Calculations and Simulations. A Hewlett Packard 9810A Calculator with a 500 step program memory was used both to evaluate rate constants and, in conjunction with a Hewlett Packard 9862A Calculator Plotter, to simulate kinetic runs.

Results

Investigation of this system was initiated at 374 and 594 nm, where product and reactant, respectively, have absorbance maxima. Preliminary results indicated that the rate of loss of reactant did not correspond to the rate of gain of product. At 594 nm, where the loss of reactant was being monitored, an initial absorbance increase was noted, followed by the expected decrease in absorbance. At 374 nm, where the gain of product was followed, there was a rapid gain in absorbance followed by a much slower absorbance increase which, at low total hydrogen peroxide concentration, lasted far longer than the time for the loss of absorbance at the other wavelength. Construction of a time-spectrum (350 - 625 nm) revealed the presence of at least one intermediate [Fig. (4)]. It was determined that this intermediate could be best studied at 500 nm, where there was apparently no interference from other absorbing species.

Figures (5) through (9) show photographs of typical kinetic traces obtained at 374, 500, and 594 nm for the indicated reaction mixtures. The kinetic trace at 374 nm consists of a fast absorbance increase followed by a very slow one. At 594 nm, where supposedly the loss of reactant is being monitored, an initial absorbance increase is noted followed by two loss steps, detectable by means of the "break" in the exponential curve. At low total hydrogen peroxide concentration, the slower of the two loss steps is over long before the termination of the slow gain at

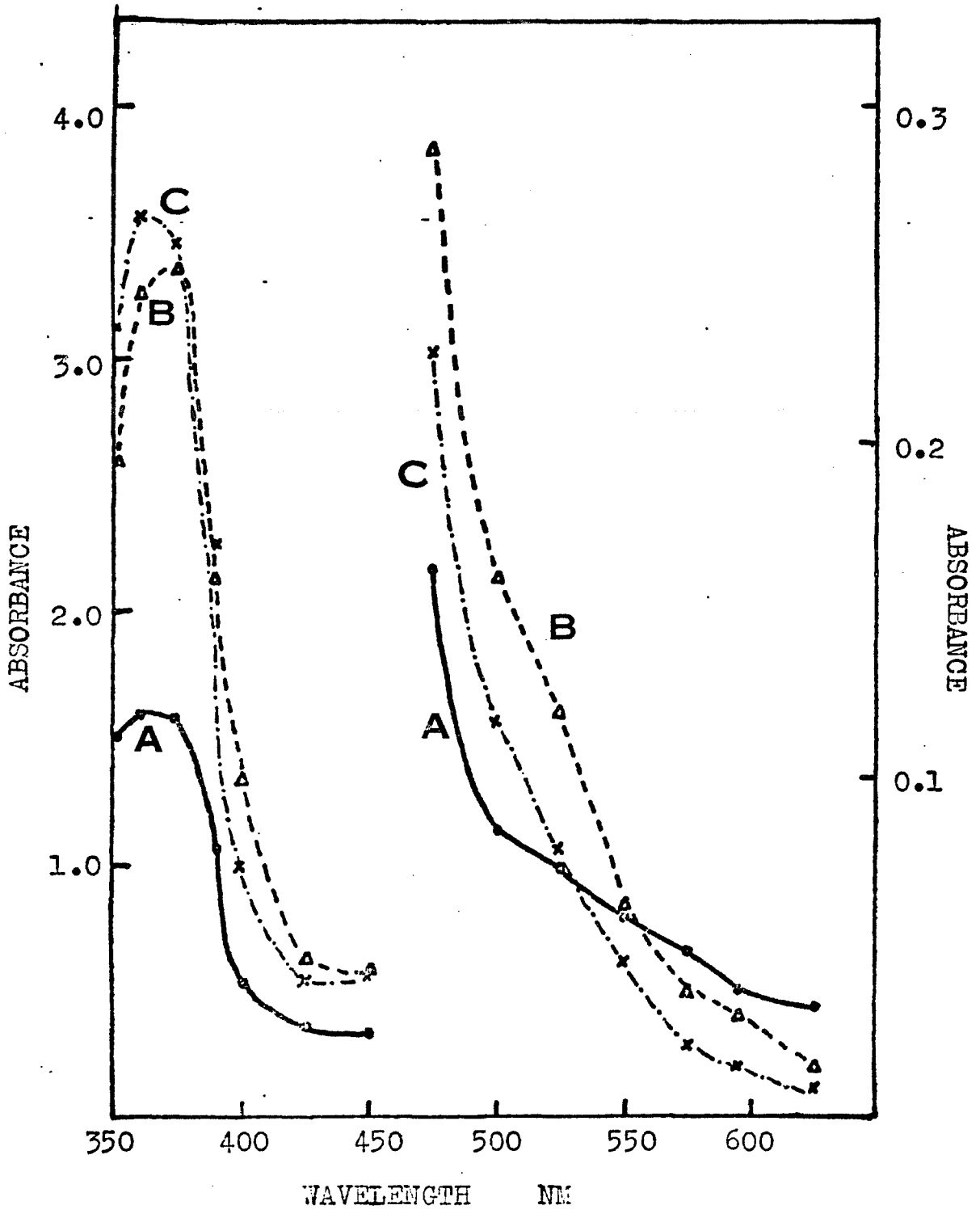

Plot of absorbance vs. wavelength for various times: A - 0.1 sec, B - 1.0 sec, C - 5.0 sec

Figure 4. Time-Spectrum.

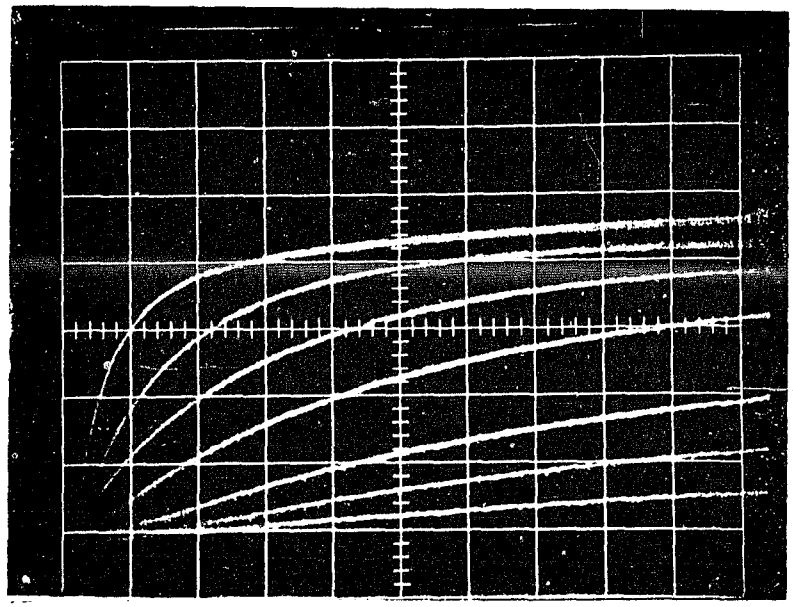

Equal amounts of reagents A and B were mixed.

Reagent A: 2.00×10^{-4} M $Cr(H_2O)_6^{3+}$; 9.76×10^{-3} M H_2O_2 ; 2.0 M $NaClO_4$

Reagent B: 0.430 M NaOH ; 2.0 M $NaClO_4$

λ = 374 nm Path Length = 10 mm 0.04 O.D./Division

Sweep Rates (from top) :
5 sec/div
2 sec/div
1 sec/div
0.5 sec/div
0.2 sec/div
0.1 sec/div
0.05 sec/div

Time Constant = 10^{-4} sec

Figure (5)

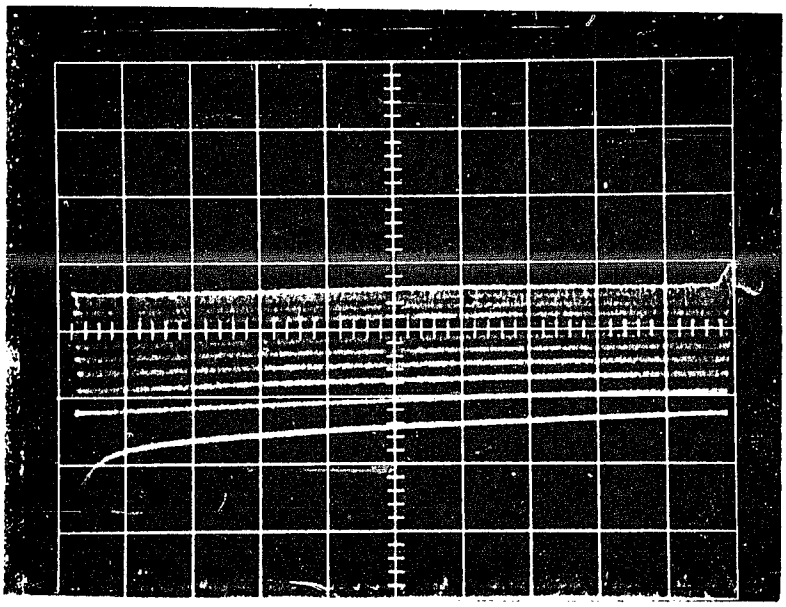

Equal amounts of reagents A and B were mixed.

Reagent A: 2.00×10^{-4} M $Cr(H_2O)_6^{3+}$; 9.76×10^{-3} M H_2O_2 ; 2.0 M $NaClO_4$

Reagent B: 0.430 M NaOH ; 2.0 M $NaClO_4$

λ = 374 nm Path Length = 10 mm 0.1 O.D./Division

Sweep Rate (reset) : 15 sec/div

Time Constant = 10^{-4} sec

Figure (6)

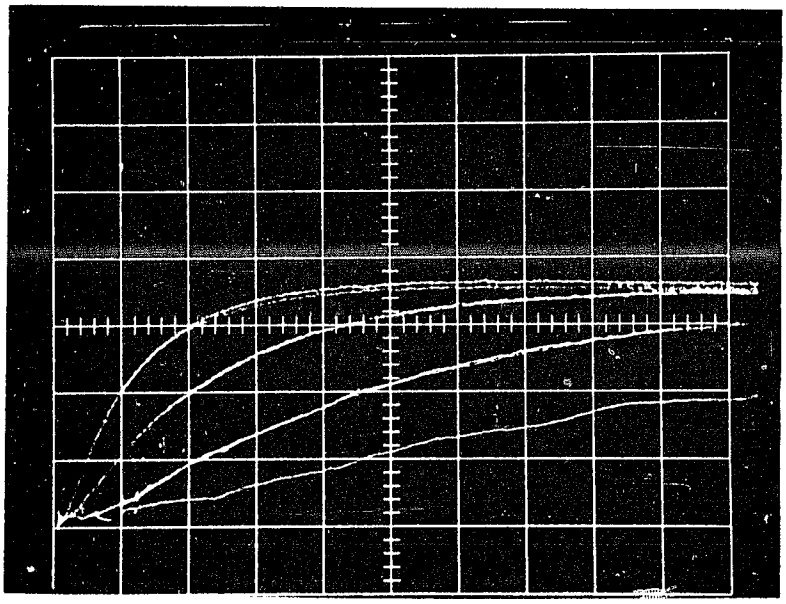

Equal amounts of reagents A and B were mixed.

Reagent A: 5.00×10^{-3} M $Cr(H_2O)_6^{3+}$; 0.195 M H_2O_2 ; 1.8 M $NaClO_4$

Reagent B: 0.782 M NaOH ; 1.8 M $NaClO_4$

λ = 500 nm Path Length = 8 mm 0.04 O.D./Division

Sweep Rates (from top) : 0.1 sec/div.
0.05 sec/div.
0.02 sec/div.
0.01 sec/div.

Time Constant = 0.001 sec

Figure (7)

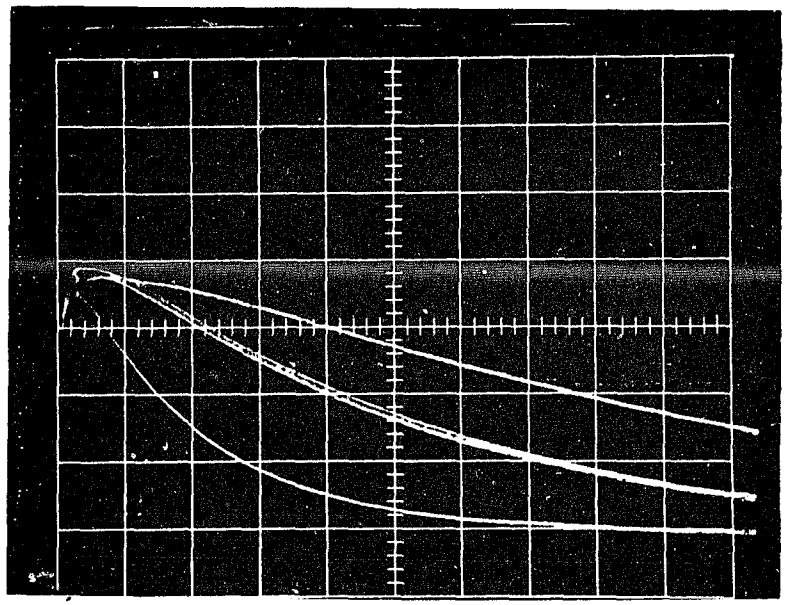

Equal amounts of reagents A and B were mixed.

Reagent A: 5.00×10^{-3} M $Cr(H_2O)_6^{3+}$; 0.195 M H_2O_2 ; 1.8 M $NaClO_4$

Reagent B: 0.782 M NaOH ; 1.8 M $NaClO_4$

λ = 500 nm Path Length = 8 mm 0.04 O.D./Division

Sweep Rates (from top) : 1 sec/div
2 sec/div
5 sec/div

Time Constant = 0.001 sec

Figure (8)

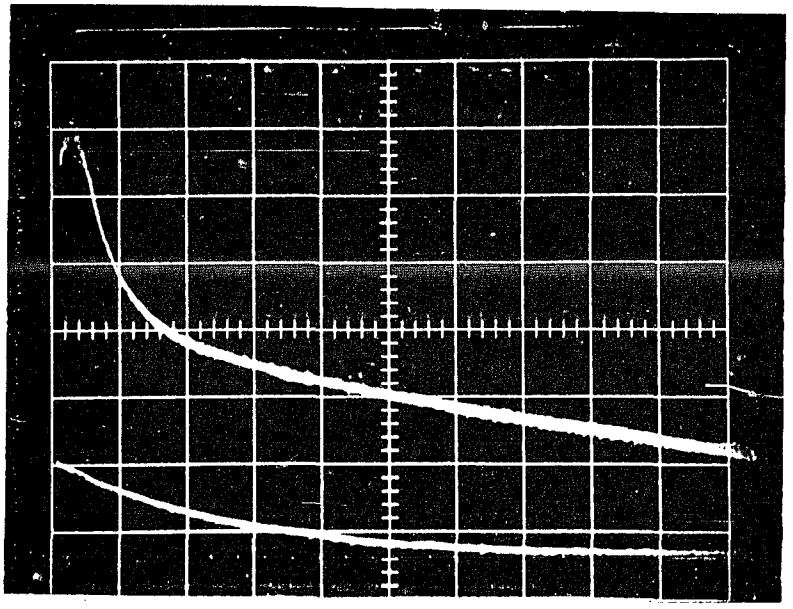

Equal amounts of reagents A and B were mixed.

Reagent A: 5.00×10^{-3} M $Cr(H_2O)_6^{3+}$; 0.0976 M H_2O_2 ; 2.1 M $NaClO_4$

Reagent B: 0.215 M NaOH ; 2.1 M $NaClO_4$

λ = 594 nm Path Length = 10 mm 0.01 O.D./Division

Sweep Rate: 1 sec/div (reset to get bottom trace)

Time Constant = 0.001 sec

Figure (9)

374 nm.

In contrast to the complications at 374 and 594 nm, the reaction at 500 nm appeared to be that of a straightforward build-up of an intermediate followed by its loss at a much slower rate. An induction period preceding the gain of intermediate, which had the effect of lengthening the time for the first half-life, was the only complexity which seemed to be present. The results obtained at 500 nm were crucial to the formulation of a mechanism for the overall process.

Kinetic Results at 500 nm. The kinetic traces obtained at this wavelength were analyzed by means of the half-life method. It was at first believed that the initial, brief induction period signified a fast reaction succeeded by a slower reaction leading to a build-up of the observed intermediate. Following this line of reasoning, analysis of kinetic runs could be carried out by neglecting the small induction period and examining the kinetic traces from points where they had become clearly exponential in form. The measured rate constants were then assumed to be due to the second step. After postulation of a mechanism and an appreciation of its mathematical implications, however, it was determined that such was not the case. The first half-life, including the induction period, was found to convey information significantly different from that conveyed by the second half-life. It thus became important to examine

both the first and second half-lives.

Columns (6) and (7) of Table (I) show the kinetic data for the first and second half-lives, respectively, for the rapid build-up of intermediate. Column (5) of Table (II) shows the data for the loss of intermediate. In all the reactions tabulated, pseudo-first-order conditions were established with chromium in limiting quantity and hydroxide in excess over hydrogen peroxide. Under these conditions the fast build-up of intermediate obeys the rate law

$$\text{Rate} = k_{obs}[\text{Cr(III)}] \quad . \tag{24}$$

The rate constant, k_{obs}, was calculated from the second half-life and can be related to the hydrogen peroxide concentration through an equation of the form

$$k_{obs} = a[H_2O_2]_T / \{1 + [OH^-]_c / b\} \tag{25}$$

where $[H_2O_2]_T$ represents the total hydrogen peroxide concentration and $[OH^-]_c$ represents the hydroxide concentration after correction for base consuming processes: conversion of $Cr(H_2O)_6^{3+}$ to CrO_2^-* and neutralization of hydrogen peroxide functioning as a monoprotic acid.

A significant feature of the kinetic traces at 500 nm is the variability of the total change in absorbance. The heights of the absorbance maxima in Table (I), column (5) (in O.D. from zero absorbance) per unit concentration of

* CrO_2^- is assumed by Baloga and Earley[21] to be the identity of the chromium(III) species initially present in basic solution.

TABLE I

KINETIC DATA AT 500 nm[a,b]

FAST GAIN

$[Cr]_T$ x 10^3	$[H_2O_2]_T$	$[OH^-]_c^c$	$[H_2O_2]^c$ x 10^4	ΔA (O.D.)	$k_{obs}^{(1)d}$ (sec^{-1})	$k_{obs}^{(2)e,f}$ (sec^{-1})
1.00	0.0293	0.407	3.16		1.5	1.7
1.00	0.0488	0.388	5.53		3.2	3.5
1.00	0.0195	0.0835	9.86	0.040	6.6	7.3
1.00	0.0975	0.340	12.5		7.7	9.2
1.00	0.0195	0.0319	23.9	0.083	11	11
1.50	0.0195	0.188	4.49	0.033	2.0	2.3
1.50	0.0195	0.103	8.08	0.053	4.1	4.6
2.50	0.0488	0.380	5.64	0.076	3.8	4.6
2.50	0.0488	0.166	12.7	0.14	8.1	8.1
2.50	0.0975	0.332	12.9	0.16	7.7	8.7
2.50	0.0975	0.283	15.1	0.17	7.7	8.7
2.50	0.184	0.235	34.2	0.30	16	21
2.50	0.0920	0.113	34.8	0.29	17	22
2.50	0.0488	0.0506	39.4	0.32	17	20
2.50	0.244	0.190	55.7	0.40	25	30

a - All runs at 25.0 ± 0.1°

b - Ionic strength is 2.2 M.

c - Calculated using the program in Appendix (II-A).

d - $k_{obs}^{(1)}$ determined from the first half-life.

e - $k_{obs}^{(2)}$ determined from the second half-life.

f - The least-squares plot of $k_{obs}^{(2)}$ vs. $[H_2O_2]$ yields $k_1 = 5.3 \times 10^3\ M^{-1}\ sec^{-1}$ as shown in Fig. (11).

TABLE II

KINETIC DATA AT 500 nm[a,b]

SLOW LOSS

$[Cr]_T$ x 10^3	$[H_2O_2]_T$	$[OH^-]_c^c$	$[H_2O_2]^c$ x 10^4	k_3 (sec^{-1})
1.00	0.0293	0.407	3.16	0.13
1.00	0.0488	0.388	5.53	0.12
1.00	0.0195	0.0835	9.86	0.085
1.00	0.0975	0.340	12.5	0.11
1.00	0.0195	0.0319	23.9	0.073
1.50	0.0195	0.188	4.49	0.083
1.50	0.0195	0.103	8.08	0.081
2.50	0.0488	0.380	5.64	0.12
2.50	0.0488	0.166	12.7	0.095
2.50	0.0975	0.332	12.9	0.12
2.50	0.0975	0.283	15.1	0.10
2.50	0.184	0.235	34.2	0.096
2.50	0.0920	0.113	34.8	0.090
2.50	0.0488	0.0506	39.4	0.076
2.50	0.244	0.190	55.7	0.13

a - All runs at 25.0 ± 0.1°

b - Ionic strength is 2.2 M.

c - Calculated using the program in Appendix (II-A).

chromium are proportional to $[H_2O_2]_T$ and inversely proportional to $[OH^-]_e$.

The observed rate constant for the slow loss of intermediate was independent of both hydrogen peroxide and hydroxide concentrations. The loss was strictly first order in intermediate as long as chromium was in limiting quantity and base was in excess of hydrogen peroxide.

Kinetic Results at 594 nm. At this wavelength, where loss of reactant should be detectable, there was a small, rapid, initial absorbance increase. The results of an experiment in which hydrogen peroxide was absent established that the gain in absorbance was not merely the consequence of mixing $Cr(H_2O)_6^{3+}$ with base. The rapid rise was followed by two successive loss steps: a rapid loss which was first order in hydrogen peroxide and chromium and inverse first order in base and a slower loss which was independent of the materials in excess. Two important observations were made at this wavelength: the total absorbance per unit concentration of chromium did not change significantly with variation of hydrogen peroxide and hydroxide concentrations over a good range, and the time taken for achievement of maximum absorbance at 594 nm was comparable to that taken for the attainment of maximum absorbance at 500 nm. No kinetic information could be obtained from the formation step. The fast loss contributed only a small increment to the total absorbance and had to be analyzed by means of the

infinite-time method [Appendix (I-B)]. The hydrogen peroxide dependence and inverse hydroxide dependence of this step was established but a precise value for the rate constant could not be determined. The slow loss step was identical to the loss step at 500 nm, having the same rate constant and being independent of the materials in excess. Table (III) contains the results for the two loss steps.

Kinetic Results at 374 nm. Table (IV) column (4) shows the rate constants for the rapid formation of intermediate at 374 nm. The fast build-up, preceded by a small induction period, follows the rate law given in equations (24) and (25) and is apparently the same process. Table (V) column (5) contains the data for the slow, hydrogen peroxide dependent step. Both steps were analyzed by the time-lag method [Appendix (I-C)]. At relatively low hydrogen peroxide concentrations, the slow step continues for a much greater amount of time than any of the loss steps observed at 500 and 594 nm.

Ionic Strength Study. An ionic strength study was carried out at 374, 500, and 594 nm in an effort to determine the nature of the net charges on the species combining to form the activated complexes in the various reactions. Tables (VI) and (VII) show the results at 500 and 594 nm and at 374 nm, respectively. Since the chromium species followed at 500 and 594 nm have relatively low absorptivities, the concentrations of reagents necessary to permit spectro-

TABLE III

KINETIC DATA AT 594 nm[a,b,c]

$[H_2O_2]_T$	$[OH^-]_c^d$	$[H_2O_2]^d$ x 10^4	ΔA (O.D.)	k_3^e (sec^{-1})	$k_5^e \times 10^{-2}$ (M^{-1} sec^{-1})
0.0488	0.0506	39.4	0.066	0.089	1.7
0.0488	0.0832	24.8	0.054	0.093	2.2
0.0488	0.166	12.7	0.055	0.11	2.5
0.0488	0.602	3.58	0.052	0.17	
0.0975	0.109	38.3	0.063	0.11	1.8
0.0975	0.166	25.5	0.056	0.11	2.1
0.0975	0.332	12.9	0.058	0.13	2.8
0.195	0.237	35.9	0.072	0.14	1.8
0.195	0.333	25.7	0.058	0.14	2.0

a - All runs have $[Cr]_T = 2.50 \times 10^{-3}$ M.

b - All runs at 25.0 ± 0.1°

c - Ionic strength is 2.2 M.

d - Calculated using the program in Appendix (II-A).

e - Evaluated by means of the infinite-time method [Appendix (I-B)]. The fast loss step, from which k_5 was evaluated, is proportional to the total hydrogen peroxide concentration and inversely proportional to the hydroxide concentration. The rate constant k_3 is independent of both hydrogen peroxide and hydroxide. Precise values of k_3 and k_5 could not be obtained as it was impossible to deconvolute the two contributing portions throughout the range of concentrations used.

TABLE IV

KINETIC DATA AT 374 nm[a,b,c]

FAST GAIN

$[H_2O_2]_T$ x 10^3	$[OH^-]_c$[d]	$[H_2O_2]$[d] x 10^5	k_{obs}[e,f] (sec^{-1})
4.88	0.0382	50.8	2.1
4.88	0.124	16.9	0.78
4.88	0.210	10.1	0.60
4.88	0.340	6.30	0.37
19.5	0.0260	285	14
19.5	0.110	75.9	3.7
19.5	0.195	43.4	2.1
19.5	0.325	26.3	1.3

a - All runs have $[Cr]_T = 1.00 \times 10^{-4}$ M.

b - All runs at 25.0 ± 0.1

c - Ionic strength is 2.2 M.

d - Calculated using the program in Appendix (II-A).

e - Evaluated by means of the time-lag method [Appendix (I-C)].

f - The least-squares plot of k_{obs} vs. $[H_2O_2]$ yields $k_1 = 4.9 \times 10^3$ M^{-1} sec^{-1} as shown in Fig. (12).

TABLE V

KINETIC DATA AT 374 nm[a,b]

SLOW GAIN

$[Cr]_T$ x 10^4	$[H_2O_2]_T$ x 10^3	$[OH^-]_c$[c]	$[H_2O_2]$[c] x 10^5	k_{obs}[d,e] x 10^3 (sec^{-1})
1.00	4.88	0.339	6.31	1.6
1.00	15.6	0.329	20.8	5.4
1.00	19.5	0.325	26.3	6.2
10.0	4.88	0.431	4.97	1.4
10.0	9.75	0.426	10.0	3.3
1.00	15.6	0.421	16.1	5.2
1.00	19.5	0.417	20.3	5.0

a - All runs at 25.0 ± 0.1°

b - Ionic strength is 2.2 M.

c - Calculated using the program in Appendix (II-A).

d - Evaluated by means of the time-lag method [Appendix (I-C)].

e - The least-squares plot of k_{obs} vs. $[H_2O_2]$ yields k_6 = 23 M^{-1} sec^{-1} as shown in Fig. (21).

TABLE VI

EFFECT OF VARIATION OF IONIC STRENGTH ON RATE CONSTANTS AT 500 AND 594 nm[a,b]

$[NaClO_4]$	μ	500 nm k_{obs}^{gain}	500 nm k_{obs}^{loss}	594 nm fast loss k_{obs} [c]
	(M)	(sec^{-1})	(sec^{-1})	(sec^{-1})
0.26	0.50	6.0	0.094	0.40
0.76	1.0	7.3	0.090	0.36
1.5	1.7	7.3	0.091	
2.0	2.2	8.5	0.095	0.28
2.5	2.7	7.9	0.10	
3.0	3.2	8.3	0.10	0.35

a - All runs have $[Cr]_T = 2.5 \times 10^{-3}$ M, $[H_2O_2]_T = 0.0488$ M $[NaOH]_T = 0.226$ M

b - All runs at 25.0 ± 0.1°

c - Evaluated by means of the infinite-time method [Appendix (I-B)]

TABLE VII

EFFECT OF VARIATION OF IONIC STRENGTH ON THE RATE CONSTANT FOR THE FAST REACTION AT 374 nm[a,b]

$[NaClO_4]$ x 10^4	μ (M)	k_{obs}[c] (sec^{-1})
4.0	0.0054	0.42
24	0.0074	0.37
54	0.010	0.42
100	0.015	0.41
150	0.020	0.48
200	0.025	0.41

a - All runs have $[Cr]_T = 2.0 \times 10^{-5}$ M, $[H_2O_2]_T = 4.86 \times 10^{-4}$ M, $[NaOH]_T = 4.89 \times 10^{-3}$ M

b - All runs at 25.0 ± 0.1°

c - Evaluated by means of the time-lag method [Appendix (I-C)]

photometric monitoring and to establish pseudo-order conditions constitute excessively high ionic strength levels.[42] The situation at 374 nm is better because the relatively high absorptivity of the species being monitored there permits the use of much lower concentrations of all reagents. No ionic strength effect was observed at any wavelength.

Effect of Carbonate. The use of sodium hydroxide to set basicity always introduces the problem of carbonate contamination. In order to minimize the amount of carbonate present, a saturated solution of sodium hydroxide (in which carbonate is only sparingly soluble) was prepared. This solution was then diluted with deaerated distilled water and stored in a polyethylene bottle.

By the analytical method mentioned in the experimental section, it was determined that, as an upper limit, the concentration of carbonate was 2.1% of the hydroxide concentration. Thus, a solution 0.431 M in hydroxide concentration is at most 0.009 M in carbonate. To determine the effect of carbonate on this system, a kinetic run was made in which a significant amount of carbonate was added.

$[Cr]_T$	$[H_2O_2]_T$	$[NaOH]_T$	$[Na_2CO_3]$	k_{obs}^{500} (sec^{-1})	k_3 (sec^{-1})	$k_5^{594} \times 10^{-2}$ ($M^{-1}sec^{-1}$)
0.0025	0.0975	0.431	---	7.5	0.11	2.6
0.0025	0.0975	0.431	0.10	6.8	0.10	2.9

These runs were made at 25.0 ± 0.1° and 2.2 M ionic strength.

The above shows that the only influence due to carbon-

ate is to effectively increase the base concentration, thereby decreasing the rate of reaction. Thus carbonate has no catalytic properties in this system.

Effect of Product. To determine the effect, if any, of chromate on the reactions being followed, several runs were made with sodium chromate added to the sodium hydroxide solution before initiation of the reaction.

$[Cr]_T$	$[H_2O_2]_T$	$[NaOH]_T$	$[CrO_4^-]$	k_{obs}^{500} (sec^{-1})	k_3 (sec^{-1})	$k_5^{594} \times 10^{-2}$ ($M^{-1}sec^{-1}$)
0.0025	0.0488	0.108	—	17	0.089	1.6
0.0025	0.0488	0.108	0.010	17	0.087	1.6
0.0025	0.0488	0.108	0.10	17	0.086	1.6

These runs were made at 25.0 ± 0.1° and 2.2 M ionic strength.

The table shows that chromate has no effect on the reactions monitored at 500 and 594 nm. No attempt was made to follow the reaction at 374 nm as chromate absorbs strongly in that region and a 0.010 M concentration of chromate would cause saturation of the PMT.

Effect of a Chelating Agent. The presence of a reaction intermediate can often be established by the effect of a chelating agent on the rate of reaction. In a study of the decomposition of peroxochromic acid by Morrow and coworkers,[43] it was observed that the addition of dipicolinic acid (DPA) to a mixture of acidified potassium dichromate and hydrogen peroxide led to a significant diminution (25 - 33%) in the

quantity of oxygen liberated over the course of an hour. This was interpreted as due to the interruption of the decomposition by the stabilization of an intermediate.

DPA could not be used in the present study due to solubility problems. Instead, ethylene diamine was added to the sodium hydroxide solution before mixing with the chromium solution.

$[Cr]_T$	$[H_2O_2]_T$	$[NaOH]_T$	[ethylene diamine]	ΔA^{500} (O.D.)	ΔA^{594} (O.D.)
0.0025	0.0975	0.441	--	0.16	0.05
0.0025	0.0975	0.441	0.25	0.024	0.04

These runs were made at 25.0 ± 0.1° and 2.2 M ionic strength.

A comparison of the two reaction mixtures, identical except for the presence of chelate in one of them, shows a drastic decrease in the maximum absorbance change at 500 nm. The effect at 594 nm is much less pronounced. It was not possible to determine any rate constants for the reactions because of excessive noise in the kinetic traces.

ESR Study. The technique of electron spin resonance spectroscopy often can supply important information on species with net electron spin angular momentum. In the present system, the +3, +4, and +5 states of chromium contain three, two, and one unpaired electron, respectively, and a priori could be expected to give rise to esr signals. There is also the possibility for signals to originate from hydroxyl and hydroperoxyl radicals (or chromium intermediates

complexed with them) generated during the course of the overall reaction.

The rapidity of the reactions to be studied by esr necessitated the use of a flow system so that monitoring of the system could take place as soon as possible after mixing. Figure (10a) shows the esr signal from a solution containing chromium(III) and hydrogen peroxide prior to mixing with base. The esr peak from a basic chromium(III) solution without hydrogen peroxide present is similarly broad. Figure (10b) shows the peak observed 0.1 second after initiation of the reaction. In addition to the obvious difference in linewidth between this peak and the one for chromium(III), it should be noted that the chromium(III) signal has completely disappeared. The rate of decay of this sharp esr peak was comparable to the rate of the slow loss step monitored spectrophotometrically at 500 nm.

The g value is often useful for identification of paramagnetic species. The region in the magnetic field where the resonance condition occurs is related to the frequency of the incident microwave radiation by the formula

$$h\nu = g\beta H_r \qquad (26)$$

where h is Planck's constant, ν is the microwave frequency, g is a factor required for all cases other than those involving pure orbital angular momentum, β is a constant called the Bohr magneton, and H_r is the resonant field strength.[44] In order to determine the g factor for the

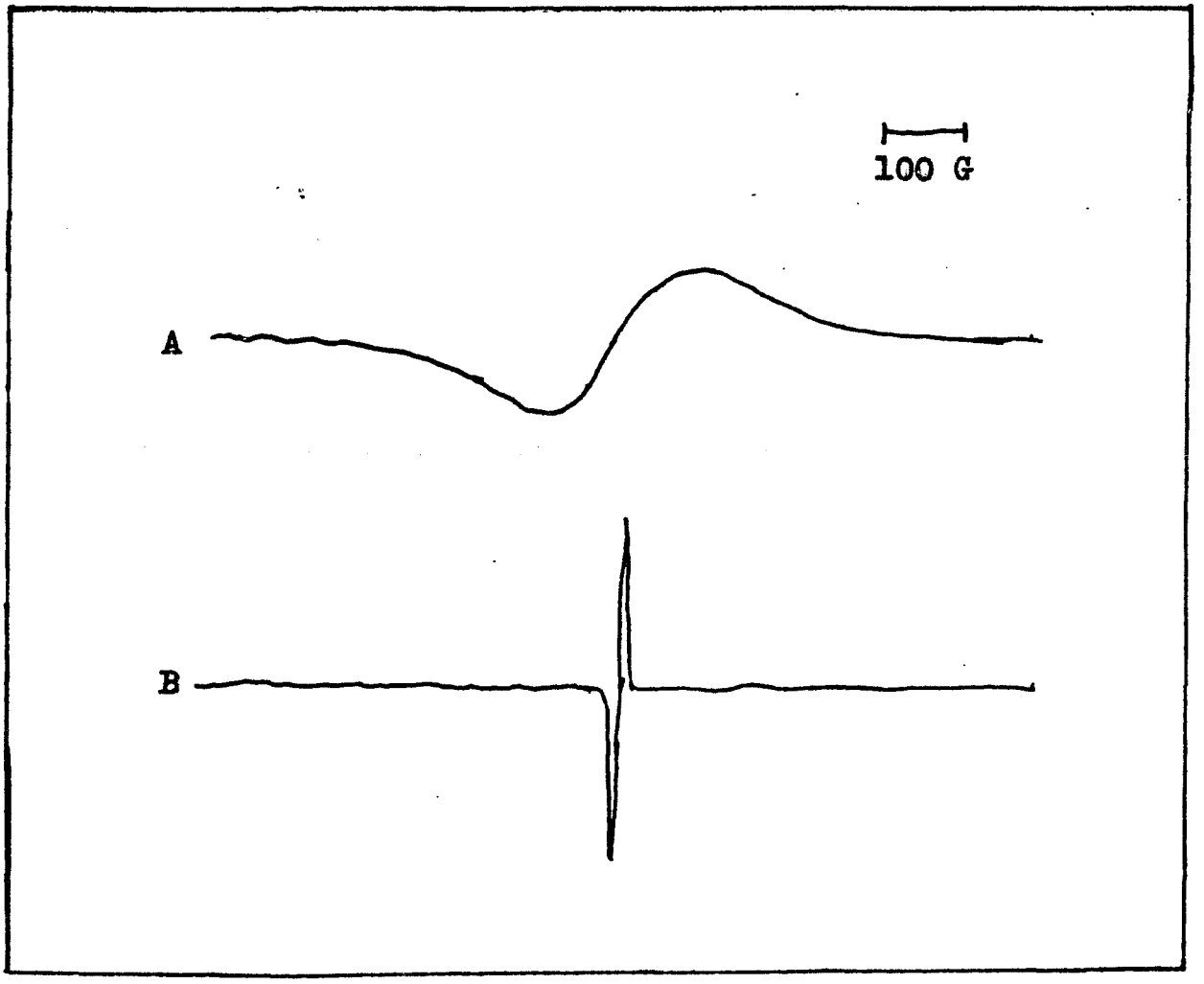

A - $[Cr]_T$ = 2.00 x 10^{-3} M, $[H_2O_2]_T$ = 0.0777 M, $[HClO_4]$ = 0.02 M

B - $[Cr]_T$ = 1.00 x 10^{-3} M, $[H_2O_2]_T$ = 0.0389 M, [NaOH] = 0.37 M

Spectrum B was recorded 0.1 second after addition of base.

Figure 10. ESR Spectra.

sharp peak observed, it was necessary to determine its position in the magnetic field relative to a standard whose g factor is known. The standard employed was solid DPPH which has a g value of 2.0037.[45] A run was made to determine the field position of the sharp DPPH peak. Then, without changing the frequency of the incident microwave radiation, the reaction was monitored and the resonant field strength at the point where the esr peak was observed was determined. Using the equation given above, the g value for the signal detected during the reaction was found to be 1.977.

The Mechanism: I. Introduction

The overall reaction obeys the following stoichiometric relationship:

$$2\ CrO_2^- + 3\ HO_2^- \longrightarrow 2\ CrO_4^{2-} + OH^- + H_2O \quad . \qquad (27)$$

A necessary preliminary in the development of a mechanism for the above is the interpretation of the hydrogen peroxide and hydroxide dependencies found for several of the reactions. There are two plausible explanations for the inverse base dependence. First, assume that the species given as CrO_2^- can be written as $Cr(OH)_4^-$ [i.e. $O^{2-} = 2(OH^-)$] and that it participates in the equilibrium

$$Cr(OH)_4^- \rightleftharpoons Cr(OH)_3 + OH^- \quad . \qquad (28)$$

If $Cr(OH)_3$ is the chemically active species, then eq. (28) combined with eq. (29)

$$Cr(OH)_3 + HO_2^- \longrightarrow Cr(O_2H)(OH)_3^- \qquad (29)$$

accounts for the observed inhibition by base. The chemically active hydrogen peroxide species is the hydroperoxide ion according to this line of reasoning.

A second explanation of the inverse hydroxide dependence is based on the assumption that hydrogen peroxide is the chemically active species. The actual hydrogen peroxide concentration, $[H_2O_2]$, is related to $[H_2O_2]_T$ and $[OH^-]_c$ through the expression

$$[H_2O_2] = [H_2O_2]_T / \left\{1 + [OH^-]_c / K_h\right\} \qquad (30)$$

where K_h is the equilibrium constant[46] for the hydrolysis of HO_2^-

$$HO_2^- + H_2O \rightleftharpoons H_2O_2 + OH^- \quad K_h = 4.44 \times 10^{-3} \qquad (31)$$

If k_{obs} of eq. (24) is related to the actual hydrogen peroxide concentration, the substitution for that concentration through eq. (30) gives an equation of the form of eq. (25).

On the basis of kinetic results alone it is not possible to distinguish between HO_2^- or H_2O_2 as the active peroxide species. Nor does an ionic strength study resolve this dilemma, for both alternatives involve neutral species. The ionic strength study did not reveal any ionic strength dependency, within the experimental error. Although not conclusive in this case because the study was outside the range of the Debye-Huckel limiting law, the absence of an ionic strength dependence is indicative of a neutral species as one of the reactants combining to form the transition state. The question remains as to whether $Cr(OH)_3$ or H_2O_2 is that neutral species.

Other workers have favored H_2O_2 as the active species. Thus, Sutin and coworkers[47] concluded that chromium(II)-cyanide complexes in basic media react much more rapidly with H_2O_2 than with HO_2^-. Their findings were in agreement with Halpern and coworkers[48] who observed that the rate of oxidation of $Co(CN)_5^{3-}$ by hydrogen peroxide exhibited an

inverse pH dependence above pH 10 which could be nicely accounted for by eq. (31). Following their lead, a similar assignment will be made of H_2O_2 as the active species in this system. Consequently, the second explanation for base inhibition will be utilized and the first explanation will be discarded.

The best starting point in the process of formulating a mechanism is to find an explanation for the dependence of the peak height at 500 nm on the hydrogen peroxide concentration given a fixed chromium concentration. The simplest mechanism which would account for this behavior is an equilibrium of the form

$$M + L \rightleftharpoons ML \tag{32}$$

$$ML \longrightarrow P \tag{33}$$

where M = chromium, L = hydrogen peroxide, ML = species absorbing at 500 nm, and P = product not absorbing at 500 nm.

In order for an intermediate to accumulate in appreciable quantity, equilibrium involving formation of ML must be established more rapidly than the rate of loss of ML to form product. The results at 500 nm further require that appreciable amounts of chromium(III) remain at equilibrium (i.e. the equilibrium lies to the left), else the change in peak height would not be too sensitive to variation in the hydrogen peroxide concentration.

The equilibrium theory can be disposed of for several reasons. First, the similarity of the slow loss steps at 500 and 594 nm suggests that one and the same species is being observed at both wavelengths. The observation that the maximum peak height at both wavelengths is achieved at the same time is also suggestive of this. Yet, in contrast to the situation at 500 nm, the peak height at 594 nm is insensitive to the variation of the hydrogen peroxide concentration. Second, the esr spectrum recorded 0.1 second after the initiation of the reaction shows no evidence of any chromium(III) species predicted to exist by the equilibrium condition. Finally, the observations made upon addition of a chelating agent are not explicable in terms of an equilibrium. The marked reduction in absorbance seen at 500 nm does not occur at 594 nm, as it must if an equilibrium is being affected.

The results at 500 and 594 nm suggest and are most readily interpretable in terms of a branching mechanism with one path being hydrogen peroxide dependent and the other path being independent of hydrogen peroxide. The mechanism can be shown schematically as

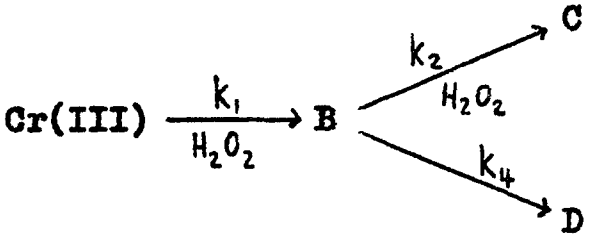

Scheme I

In the above mechanism only species C absorbs at 500 nm

whereas both species C and D absorb (with similar absorptivities) at 594 nm. The presence of species B is necessary to explain the induction period observed at 374 and 500 nm. Also, if this preliminary step were omitted, the absence of an intermediate B whose formation is hydrogen peroxide dependent would imply that D is formed whether or not hydrogen peroxide is present in a basic chromium solution, which is not the case. According to this scheme, variation in the hydrogen peroxide concentration will directly influence the amount of C produced relative to D with a concommitant effect on the absorbance at 500 nm. No such effect on absorbance will be seen at 594 nm since any decrease in C merely increases D and vice versa.

The branching mechanism explains the effect seen upon addition of chelate in a very simple manner. The chelate has lowered the amount of C produced so that the absorbance at 500 nm is considerably reduced. The production of D rises in direct consequence of the diminution of C so that the absorbance at 594 nm is not greatly affected. It is eminently reasonable that C should be reduced in concentration relative to D - the hydrogen peroxide molecule which must coordinate to produce C is blocked by the chelating ligand.

The esr result is evidence that all of the chromium(III) has been consumed prior to the time of monitoring.

The presence of two loss steps at 594 nm is easily accounted for by this mechanism. Since two species, C and D,

are being produced and are visible at 594 nm, it is not unreasonable for them to decay by different mechanisms at different rates.

The Mechanism: II. Mathematical Development

The reactions observed at 500 nm are the key to an understanding of the overall reaction process. A representation more complete than that given by Scheme I is

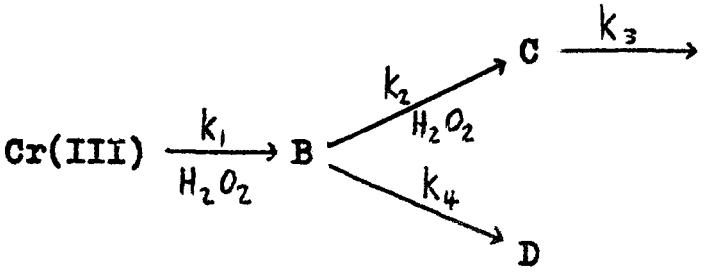

Scheme II

where k_3 is the rate constant for the slow loss step. The mathematical consequences of this mechanism, focusing on species C, will be explored at this point.

The relevant differential rate equations characterizing this system with time are:

$$-d[Cr(III)]/dt = k_1[H_2O_2][Cr(III)] \quad (34)$$

$$-d[B]/dt = -k_1[H_2O_2][Cr(III)] + (k_2[H_2O_2] + k_4)[B] \quad (35)$$

$$-d[C]/dt = -k_2[H_2O_2][B] + k_3[C] \quad (36)$$

The variation of the concentration of D with time does not have to be treated in this development of the mathematics.

One of the standard mathematical techniques[49,50] for solving such a set of equations is to assume that the following trial solutions hold:

$$[Cr(III)] = ae^{-mt} \quad (37)$$

$$[B] = be^{-mt} \quad (38)$$

$$[C] = ce^{-mt} \tag{39}$$

Substitution of the trial solutions into their respective differential equations, followed by rearrangement yields

$$(m - k_1[H_2O_2])a = 0 \tag{40}$$

$$(m - k_2[H_2O_2] - k_4)b + k_1[H_2O_2]a = 0 \tag{41}$$

$$(m - k_3)c + k_2[H_2O_2]b = 0 \tag{42}$$

The method of determinants is now applied to solve the above linear simultaneous equations.

$$\begin{vmatrix} m - k_1[H_2O_2] & 0 & 0 \\ k_1[H_2O_2] & m - k_2[H_2O_2] - k_4 & 0 \\ 0 & k_2[H_2O_2] & m - k_3 \end{vmatrix} = 0$$

Expansion of the determinant gives the equation

$$(m - k_1[H_2O_2])(m - k_2[H_2O_2] - k_4)(m - k_3) = 0 \tag{43}$$

the roots of which are

$$m_1 = k_1[H_2O_2] \quad m_2 = k_2[H_2O_2] + k_4 \quad m_3 = k_3 .$$

These three roots, when applied to the original trial solutions [eqs. (37), (38), and (39)], generate a set of three simultaneous equations

$$[Cr(III)] = a_1e^{-m_1t} + a_2e^{-m_2t} + a_3e^{-m_3t} \tag{44}$$

$$[B] = b_1 e^{-m_1 t} + b_2 e^{-m_2 t} + b_3 e^{-m_3 t} \tag{45}$$

$$[C] = c_1 e^{-m_1 t} + c_2 e^{-m_2 t} + c_3 e^{-m_3 t} \tag{46}$$

There is enough information available to turn the above expressions into explicit equations permitting the calculation of each concentration as a function of time.

Setting $t = 0$,

$$[Cr(III)] = [Cr(III)]_T = a_1 + a_2 + a_3 \tag{47}$$

$$[B] = [B]_o = 0 = b_1 + b_2 + b_3 \tag{48}$$

$$[C] = [C]_o = 0 = c_1 + c_2 + c_3 \tag{49}$$

Substituting the various values for m into eq. (40), it becomes apparent that $a_2 = a_3 = 0$ [viz. $(m_2 - k_1[H_2O_2])a_2 = 0$, and since $m_2 - k_1[H_2O_2] \neq 0$, then a_2 must equal zero] and [from eq. (47)] $a_1 = [Cr(III)]_T$. Therefore, substituting into eq. (44) yields

$$[Cr(III)] = [Cr(III)]_T e^{-k_1[H_2O_2]t} \tag{50}$$

Evaluating eq. (41) in an analogous fashion leads to

$$b_1 = \frac{k_1[H_2O_2]a_1}{(k_2 - k_1)[H_2O_2] + k_4} \tag{51}$$

and $b_3 = 0$. Utilizing eq. (48), it follows that $b_1 = -b_2$ and eq. (45) becomes

$$[B] = \frac{k_1[H_2O_2][Cr(III)]_T}{(k_2 - k_1)[H_2O_2] + k_4}\left\{e^{-k_1[H_2O_2]t} - e^{-(k_2[H_2O_2] + k_4)t}\right\} \quad (52)$$

Equations (42) and (49) provide the following relationships:

$$(k_1[H_2O_2] - k_3)c_1 + k_2[H_2O_2]b_1 = 0 \quad (53)$$

$$(k_2[H_2O_2] + k_4 - k_3)c_2 + k_2[H_2O_2]b_2 = 0 \quad (54)$$

$$c_3 = - c_1 - c_2 \quad (55)$$

Solving for the values of c_1, c_2, and c_3 through these equations and substituting them into eq. (46) results, upon rearrangement, in the following expression for the concentration of species C at any time:

$$[C] = - \frac{k_1k_2[H_2O_2]^2[Cr(III)]_T \; e^{-k_1[H_2O_2]t}}{\left\{(k_2 - k_1)[H_2O_2] + k_4\right\}(k_1[H_2O_2] - k_3)} + \frac{k_1k_2[H_2O_2]^2[Cr(III)]_T \; e^{-(k_2[H_2O_2] + k_4)t}}{\left\{(k_2 - k_1)[H_2O_2] + k_4\right\}(k_2[H_2O_2] + k_4 - k_3)} + \frac{k_1k_2[H_2O_2]^2[Cr(III)]_T \; e^{-k_3t}}{(k_1[H_2O_2] - k_3)(k_2[H_2O_2] + k_4 - k_3)} \quad (56)$$

It will be shown later that, during the formation of C and at the time at which the maximum amount of C is formed, the loss step represented by k_3 can be neglected. Equation (56) then reduces to

$$[C] = \frac{k_2[H_2O_2][Cr(III)]_T}{k_2[H_2O_2] + k_4} - \frac{k_2[H_2O_2][Cr(III)]_T \; e^{-k_1[H_2O_2]t}}{(k_2 - k_1)[H_2O_2] + k_4}$$

$$+ \frac{k_1k_2[H_2O_2]^2[Cr(III)]_T \; e^{-(k_2[H_2O_2] + k_4)t}}{\{(k_2 - k_1)[H_2O_2] + k_4\}(k_2[H_2O_2] + k_4)} \qquad (57)$$

and the maximum concentration of C (setting $t = \infty$ and ignoring the loss step) is

$$[C]_{max} = \frac{k_2[H_2O_2][Cr(III)]_T}{k_2[H_2O_2] + k_4} \qquad (58)$$

Equation (58) is a particularly useful expression. Its first application will be to help relate the observed rate constants at 500 nm to the microscopic rate constants presented in Scheme II.

The time elapsed for the absorbance to reach half of the maximum value is called the first half-life. The first half-life at 500 nm is unique in that it includes the induction period and is thus longer than subsequent half-lives. Since the concentration of C at the first half-life, $[C]_{\frac{1}{2}}$, is one-half the maximum concentration, eqs. (57) and (58) can be related in the following manner:

$$[C]_{\frac{1}{2}} = \tfrac{1}{2}[C]_{max} = \frac{1}{2}\frac{k_2[H_2O_2][Cr(III)]_T}{k_2[H_2O_2] + k_4}$$

$$= \frac{k_2[H_2O_2][Cr(III)]_T}{k_2[H_2O_2] + k_4} - \frac{k_2[H_2O_2][Cr(III)]_T \; e^{-k_1[H_2O_2]t_{\frac{1}{2}}(1)}}{(k_2 - k_1)[H_2O_2] + k_4}$$

$$+ \frac{k_1 k_2 [H_2O_2]^2 [Cr(III)]_T \; e^{-(k_2[H_2O_2] + k_4)t_{\frac{1}{2}}(1)}}{\{(k_2 - k_1)[H_2O_2] + k_4\}(k_2[H_2O_2] + k_4)} \qquad (59)$$

The first half-life is designated by $t_{\frac{1}{2}}(1)$.

If k_1 is a rate constant for a process much slower than processes represented by k_2 and k_4 such that

$$k_1[H_2O_2] \ll k_2[H_2O_2] + k_4 \ ,$$

then

$$e^{-k_1[H_2O_2]t_{\frac{1}{2}}(1)} \gg \frac{k_1[H_2O_2] \; e^{-(k_2[H_2O_2] + k_4)t_{\frac{1}{2}}(1)}}{k_2[H_2O_2] + k_4} \ .$$

The validity of this assumption will be shown later. Using this assumption in eq. (59) gives rise to the expression

$$\frac{1}{2} \frac{k_2[H_2O_2][Cr(III)]_T}{k_2[H_2O_2] + k_4} = \frac{k_2[H_2O_2][Cr(III)]_T}{k_2[H_2O_2] + k_4} - \frac{k_2[H_2O_2][Cr(III)]_T \; e^{-k_1[H_2O_2]t_{\frac{1}{2}}(1)}}{(k_2 - k_1)[H_2O_2] + k_4} \qquad (60)$$

which upon rearrangement and taking logarithms yields

$$k_{obs}^{(1)} = \frac{\ln 2}{t_{\frac{1}{2}}(1)} = \frac{-k_1[H_2O_2] \ln 2}{\ln\left[\frac{1}{2}\left(1 - \frac{k_1[H_2O_2]}{k_2[H_2O_2] + k_4}\right)\right]} \qquad (61)$$

where $k_{obs}^{(1)}$ is calculated from the relationship between the rate constant and the half-life for a first-order reaction.

At the time, $t_{3/4}$, when three-quarters of the height of maximum absorbance has been achieved, the concentration of C is

$$[C]_{3/4} = \frac{3}{4}\frac{k_2[H_2O_2][Cr(III)]_T}{k_2[H_2O_2] + k_4} = \frac{k_2[H_2O_2][Cr(III)]_T}{k_2[H_2O_2] + k_4}$$

$$- \frac{k_2[H_2O_2][Cr(III)]_T \; e^{-k_1[H_2O_2]t_{3/4}}}{(k_2 - k_1)[H_2O_2] + k_4} \qquad (62)$$

with the assumption that $e^{-(k_2[H_2O_2] + k_4)t_{3/4}}$ is negligible.

Rearrangement of eq. (62) gives

$$e^{-k_1[H_2O_2]t_{3/4}} = \frac{1}{4}\frac{(k_2 - k_1)[H_2O_2] + k_4}{k_2[H_2O_2] + k_4} \qquad (63)$$

which, upon the taking of logarithms and further rearrangement, results in

$$t_{3/4} = -\frac{1}{k_1[H_2O_2]} \ln\left[\frac{1}{4}\left(1 - \frac{k_1[H_2O_2]}{k_2[H_2O_2] + k_4}\right)\right] . \qquad (64)$$

From eq. (61)

$$t_{\frac{1}{2}}(1) = -\frac{1}{k_1[H_2O_2]} \ln\left[\frac{1}{2}\left(1 - \frac{k_1[H_2O_2]}{k_2[H_2O_2] + k_4}\right)\right] . \qquad (65)$$

Subtraction of eq. (65) from eq. (64) gives

$$t_{3/4} - t_{\frac{1}{2}}(1) = \frac{1}{k_1[H_2O_2]}\left\{\ln\left[\frac{1}{2}\left(1 - \frac{k_1[H_2O_2]}{k_2[H_2O_2] + k_4}\right)\right]\right.$$

$$\left. - \ln\left[\frac{1}{4}\left(1 - \frac{k_1[H_2O_2]}{k_2[H_2O_2] + k_4}\right)\right]\right\} \qquad (66)$$

or

$$t_{3/4} - t_{\frac{1}{2}}^{(1)} = \frac{\ln 2}{k_1[H_2O_2]} \quad . \tag{67}$$

The quantity $t_{3/4} - t_{\frac{1}{2}}^{(1)}$ is actually the second half-life, $t_{\frac{1}{2}}^{(2)}$, and therefore

$$k_{obs}^{(2)} = \frac{\ln 2}{t_{\frac{1}{2}}^{(2)}} = k_1[H_2O_2] \quad . \tag{68}$$

The mathematics predicts that the third and subsequent half-lives should equal the second half-life.

Extension of the mechanism to encompass experimental observations made at 374 and 594 nm leads to the following overall formulation:

Scheme III

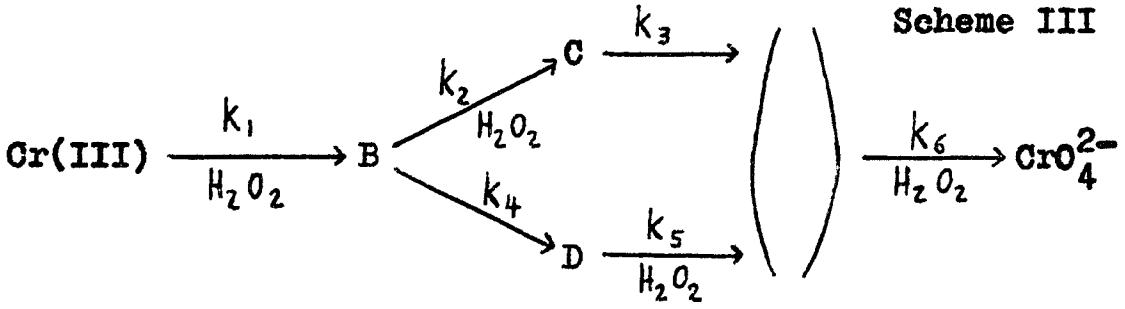

The parentheses indicate an intermediate(s) which could not be monitored.* The rate constant k_5 is for the fast loss of intermediate observable at 594 nm. The rate constant k_6 represents the slow process monitored at 374 nm.

From the above mechanism, it can be seen that the interpretation of the kinetics observed at 500 nm is central to an understanding of this system. The subsequent reactions are straightforward in terms of their kinetic

* The necessity for such will be explained later.

interpretation. The thrust of the next section will therefore be to test the equations pertaining to Scheme II.

The Mechanism: III. Experimental Verification

The mathematics derived from Scheme II and the three assumptions (the fast processes at 374 and 500 nm are one and the same, $k_1[H_2O_2] \ll k_2[H_2O_2] + k_4$, and the gain and loss steps at 500 nm are decoupled) can now be tested. With the twin assumptions that the formation of B is the rate-determining step and that the rapid gains in absorbance observed at 374 and 500 nm are due to the same process, the value of the rate constant k_1 should be experimentally accessible through the second half-life [from eq. (68)] at either wavelength. The least-squares plot of $k_{obs}^{(2)}$ vs. $[H_2O_2]$ for the data at 500 nm [shown in Fig. (11)] is linear, as predicted, with a slope of 5.3×10^3 M^{-1} sec^{-1}.* The prediction made in the previous section that the third and subsequent half-lives would equal the second half-life was borne out at 500 nm. The earliest parts of the kinetic traces at 374 nm could not be analyzed by the half-life method because of complications arising from the presence of the subsequent slow absorbance increase. The data was analyzed by the time-lag method and the least-squares plot of k_{obs} vs. $[H_2O_2]$ [shown in Fig. (12)] is linear with a slope of 4.9×10^3 M^{-1} sec^{-1}. This is within the experimental error and is in good agreement with the result at 500 nm, for a smaller k_1 value is expected at 374 nm because of the influence of the induction period on the portions of the traces analyzed. Thus the assumption that the fast

* The significance of the intercept will be discussed later.

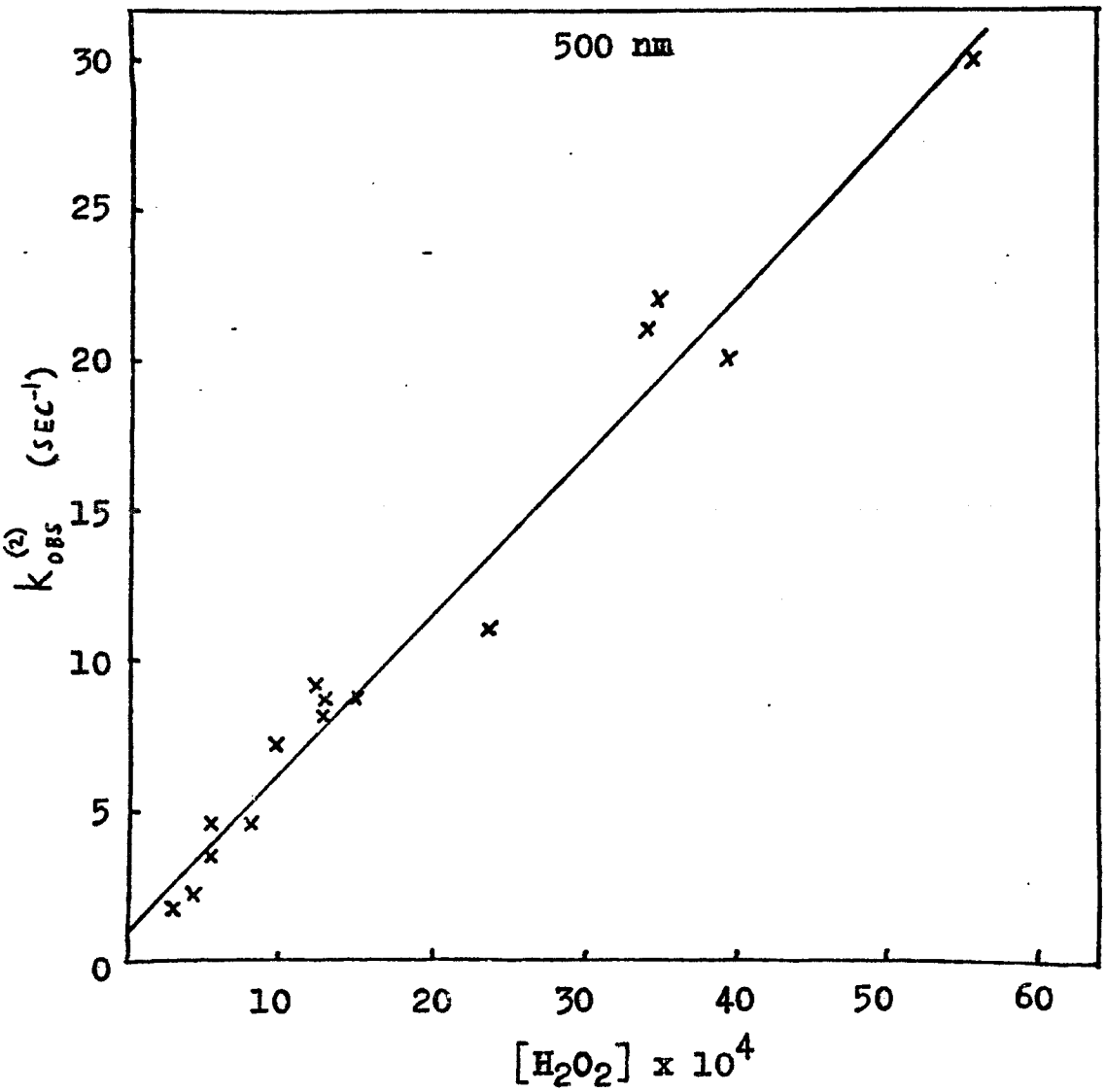

This graph is based on the data in Table (I).

The equation for the straight line, calculated by the method of least-squares, is

$$k_{obs}^{(2)} = 0.98 + 5.3 \times 10^3 [H_2O_2]$$

Figure 11. Plot of $k_{obs}^{(2)}$ vs. $[H_2O_2]$.
Formation step at 500 nm.

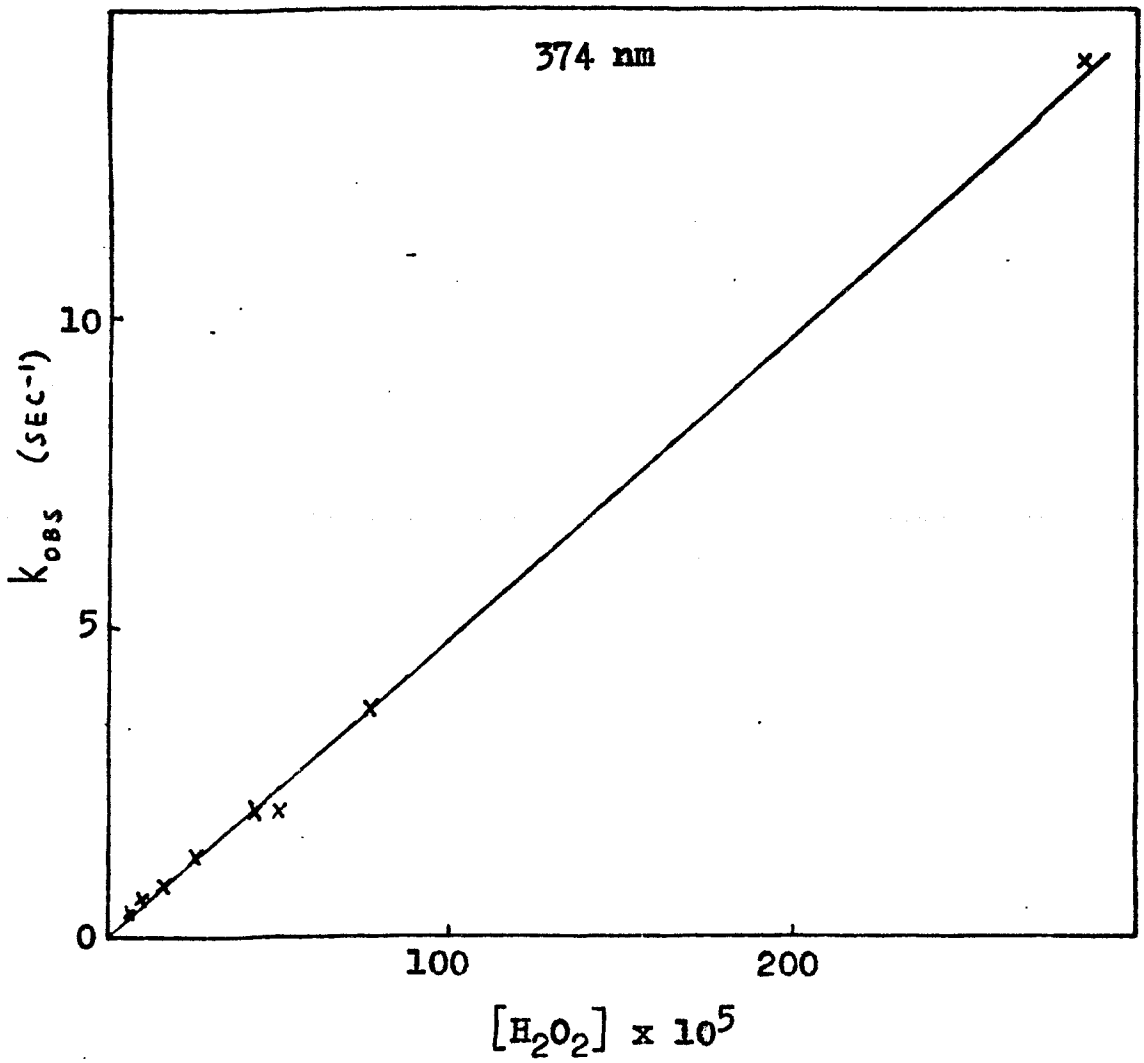

This graph is based on the data in Table (IV).

The equation for the straight line, calculated by the method of least-squares, is

$$k_{obs} = -0.040 + 4.9 \times 10^3 [H_2O_2]$$

Figure 12. Plot of k_{obs} vs. $[H_2O_2]$.
The fast reaction at 374 nm.

processes followed at 374 and 500 nm are one and the same is seen to hold.

Since k_2 and k_4 cannot be measured directly (as $k_2 \gg k_1$ and the formation of D cannot be followed without interference from C at 594 nm), eq. (58) will be utilized both as a test of the mechanism and to gain some information on these rate constants. The concentration $[C]_{max}$ in eq. (58) is not known since k_2 and k_4 are not known, but it can be related to an observable physical property - the absorbance. Assuming that species C obeys Beer's law, $[C]_{max} = \Delta A/\epsilon$ for unit path length. ΔA is the maximum change in absorbance and ϵ is the absorptivity of species C at 500 nm. Substitution into eq. (58) and rearrangement results in the relationship

$$\frac{\epsilon[Cr(III)]_T}{\Delta A} = 1 + \frac{k_4}{k_2[H_2O_2]} \quad . \tag{69}$$

Figure (13) shows the least-squares plot of the term $[Cr(III)]_T/\Delta A$ vs. $1/[H_2O_2]$. The linearity provides excellent support for the branching mechanism. The value of ϵ (= 310) was chosen to give an intercept of one. The resultant slope is the ratio $k_4:k_2$ (= 0.0056).

The assumption made prior to eq. (60) can now be tested. If the opposite assumption is made (i.e. $k_1[H_2O_2] \gg k_2[H_2O_2] + k_4$) then, following the same procedure used to derive eqs. (64) and (65), there are obtained

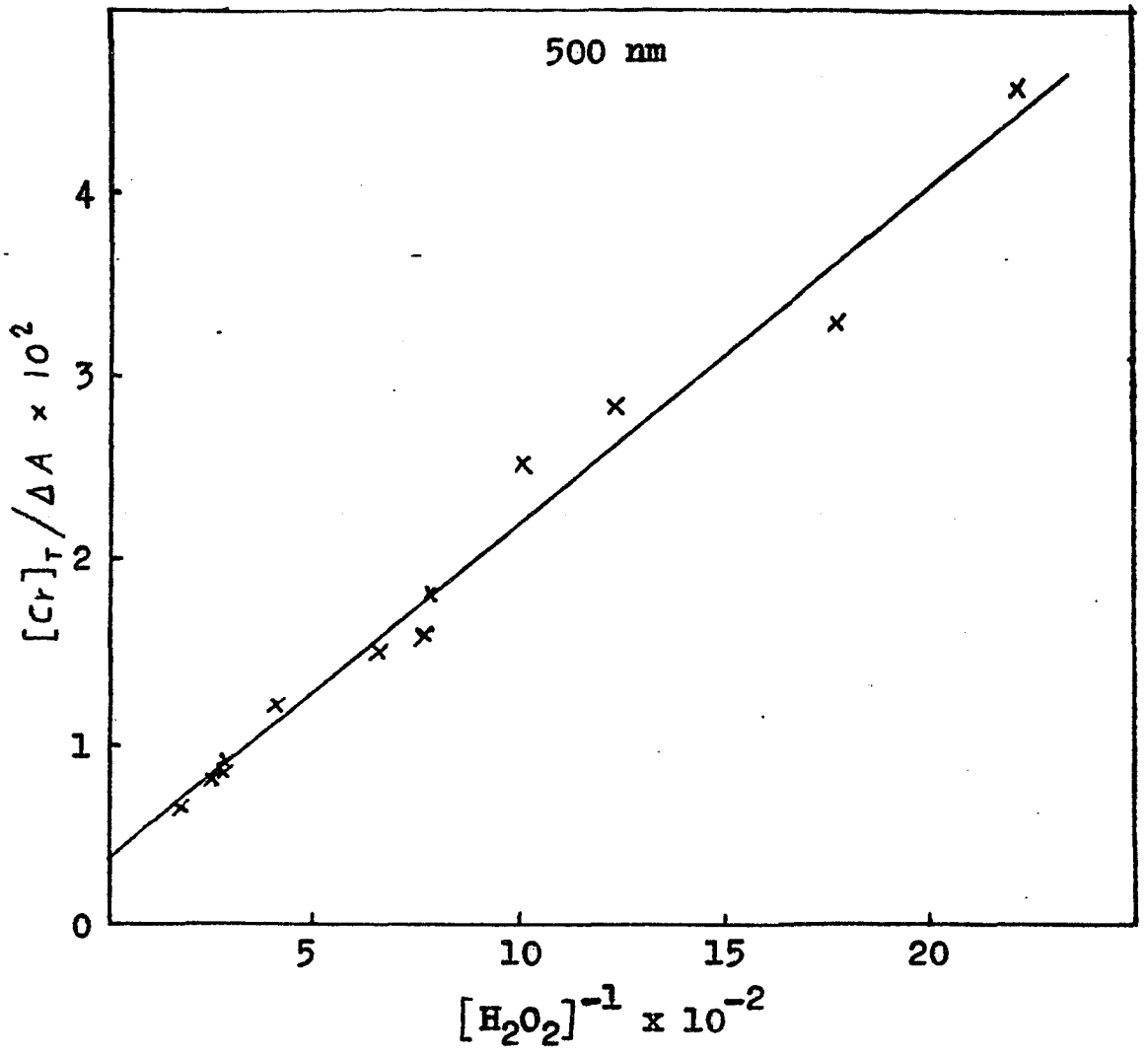

This graph is based on the data in Table (I) and on eq. (69). The equation for the straight line, calculated by the method of least-squares, is

$$[Cr]_T/\Delta A = 3.2 \times 10^{-3} + 1.8 \times 10^{-5}[H_2O_2]^{-1} .$$

Multiplication of both sides of the above equation by 310 sets the intercept equal to one, as required by eq. (69), and gives an adjusted slope of 0.0056. The factor 310 is the absorptivity of the intermediate and the adjusted slope is the ratio k_4/k_2.

Figure 13. Test of the Branching Mechanism.

$$t_{\frac{1}{2}}^{(1)} = -\frac{1}{k_2[H_2O_2] + k_4} \ln\left[\frac{1}{2}\left(1 - \frac{k_2[H_2O_2] + k_4}{k_1[H_2O_2]}\right)\right] \qquad (70)$$

and

$$t_{3/4} = -\frac{1}{k_2[H_2O_2] + k_4} \ln\left[\frac{1}{4}\left(1 - \frac{k_2[H_2O_2] + k_4}{k_1[H_2O_2]}\right)\right] . \qquad (71)$$

Subtraction of eq. (70) from eq. (71) gives

$$t_{3/4} - t_{\frac{1}{2}}^{(1)} = \frac{\ln 2}{k_2[H_2O_2] + k_4} . \qquad (72)$$

Once again, the quantity $t_{3/4} - t_{\frac{1}{2}}^{(1)}$ is actually the second half-life, $t_{\frac{1}{2}}^{(2)}$, so that

$$k_{obs}^{(2)} = \frac{\ln 2}{t_{\frac{1}{2}}^{(2)}} = k_2[H_2O_2] + k_4 \qquad (73)$$

The plot of $k_{obs}^{(2)}$ vs. $[H_2O_2]$ shown in Fig. (11) yielded a value of 0.98 for the intercept and a value of 5.3×10^3 for the slope. Equation (73) identifies the slope with k_2 and the intercept with k_4. The ratio $k_4:k_2 = 0.00019$ thus obtained is in sharp contrast to the value determined through eq. (69). The value there is 0.0056 which is nearly thirty times as great. It must be remembered that eq. (69) was derived without any assumptions being made concerning the relative magnitudes of k_1, k_2, and k_4. Therefore, the assumption that $k_2[H_2O_2] + k_4 \ll k_1[H_2O_2]$ leading to eq. (73) is rejected.

Although eq. (68) does not predict an intercept for

the plot of $k_{obs}^{(2)}$ vs. $[H_2O_2]$, there is no real discrepancy. The intercept [Fig. (11)] can be explained as being due to a small dependence on the hydroperoxide concentration. A least-squares analysis of the function $k_{obs}^{(2)} = f_1 + f_2[H_2O_2] + f_3[HO_2^-]$ showed it to be linear with a high correlation but the coefficients were unreliable due to the magnitude of the experimental error. The small negative intercept for the plot of k_{obs} vs. $[H_2O_2]$ for the data at 374 nm [Fig. (12)] is also a result of the experimental error. The assumption that $k_1[H_2O_2] \sim k_2[H_2O_2] + k_4$ leads to a complicated expression for the half-lives which cannot be resolved.

In order to determine individual values for the rate constants k_2 and k_4, a calculator program for the simulation of kinetic traces was written [Appendix (II-B)] based on eq. (56). Using the values of k_1 and ϵ determined previously and varying k_2 and hence k_4 (with $k_4/k_2 = 0.0056$) until the best traces were obtained, values for k_2 and k_4 were determined. Simulations with experimental points indicated to facilitate comparison are presented for the rapid gain at 500 nm in Figs. (14) - (17).

The assumption that the fast gain and slow loss steps at 500 nm are decoupled, permitting k_3 to be neglected for the build-up, will now be explained. Figures (18) and (19) show simulations of the loss step at 500 nm. Note that the simulated kinetic traces parallel the experimental traces but are displaced in time. The explanation is a delay caused by a second induction period. The species C is being lost

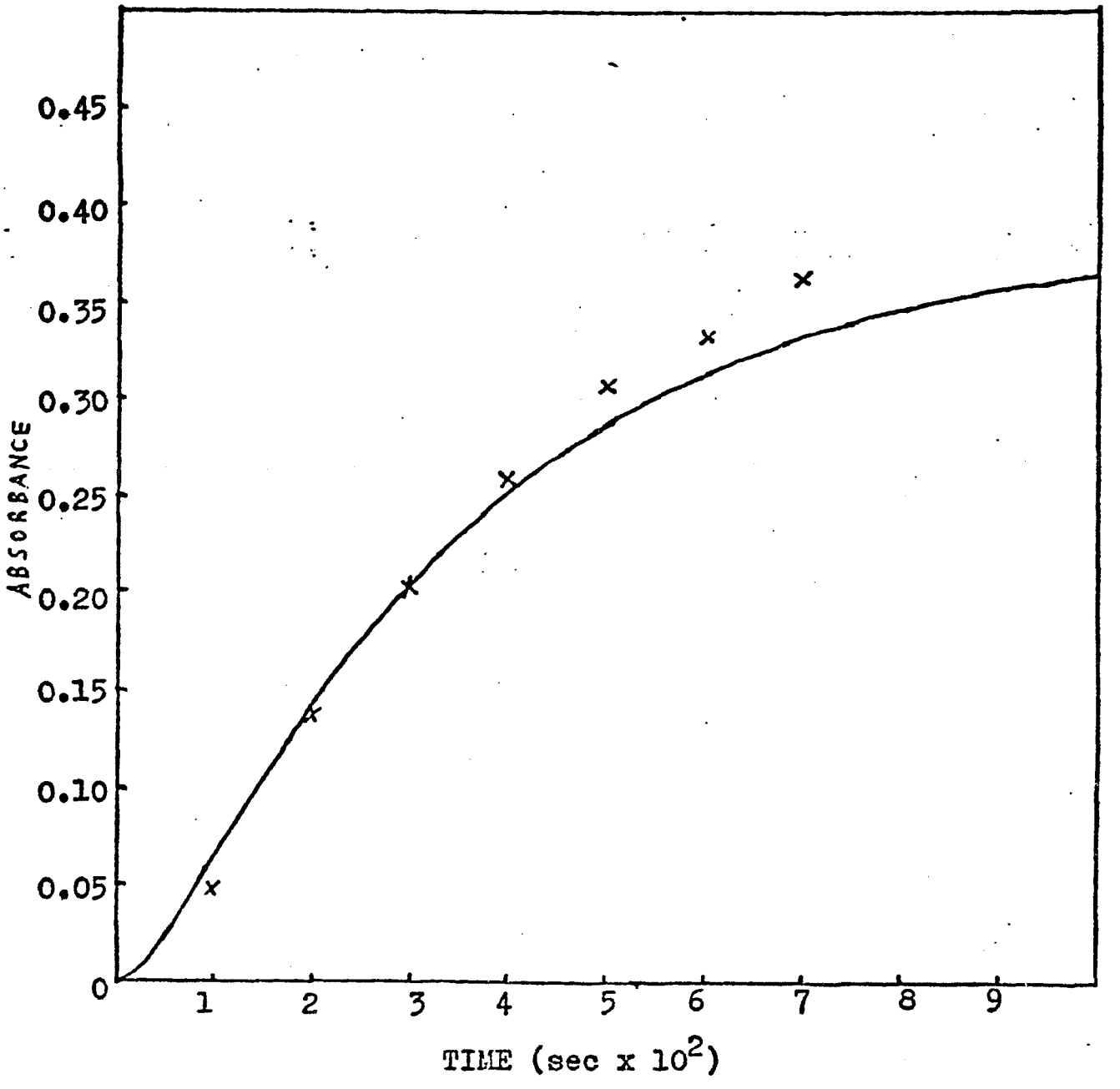

$[Cr]_T = 2.50 \times 10^{-3}$ M, $[H_2O_2] = 5.57 \times 10^{-3}$ M, $k_3 = 0.13$ sec^{-1}
Values for all other variables are given in Appendix (II-B), which contains the program for plotting the simulated kinetic trace. The crosses indicate experimental points.

Figure 14. Simulation of a Kinetic Trace.

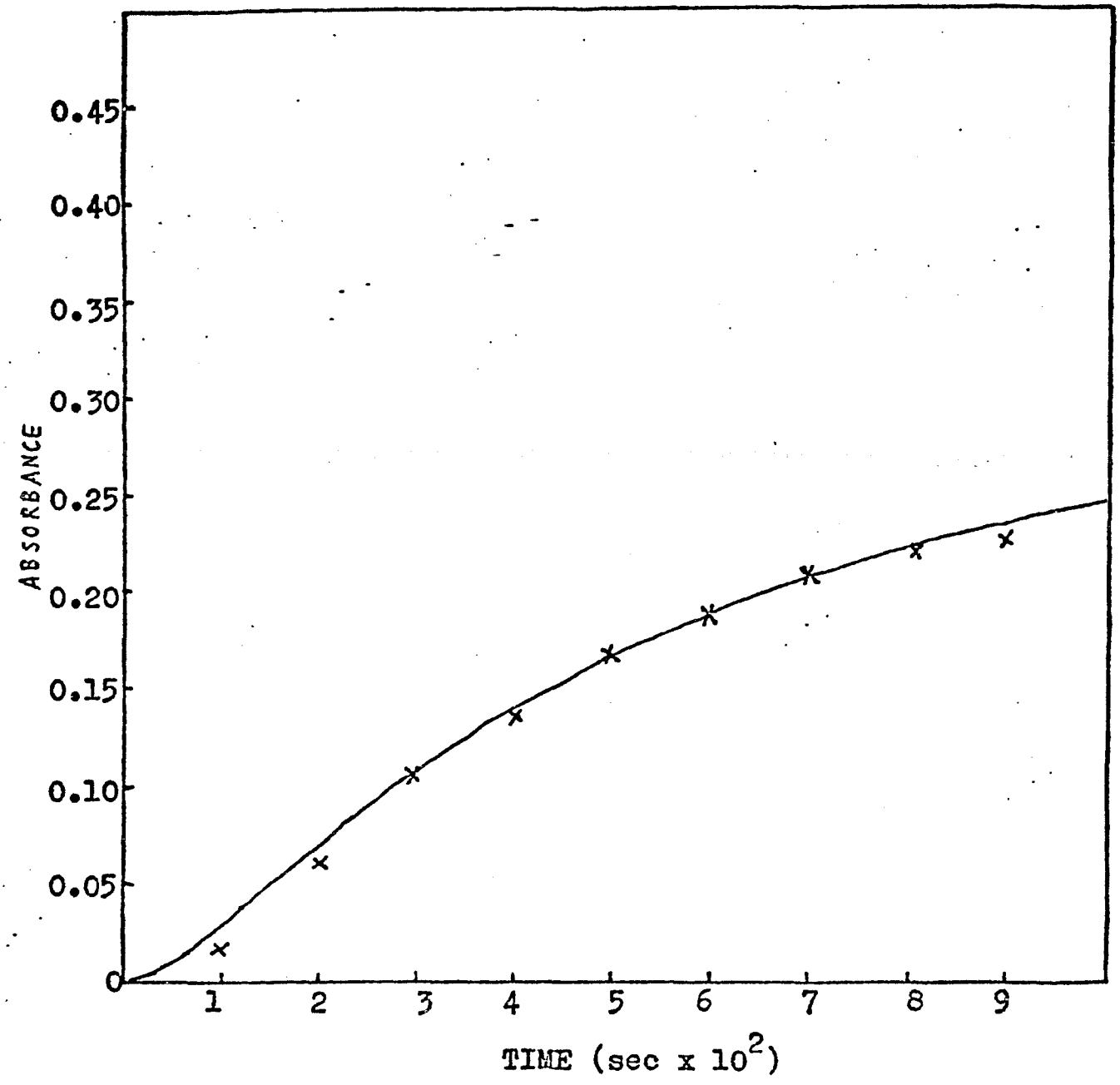

$[Cr]_T = 2.50 \times 10^{-3}$ M, $[H_2O_2] = 3.48 \times 10^{-3}$ M, $k_3 = 0.090$ sec^{-1}
Values for all other variables are given in Appendix (II-B), which contains the program for plotting the simulated kinetic trace. The crosses indicate experimental points.

Figure 15. Simulation of a Kinetic Trace.

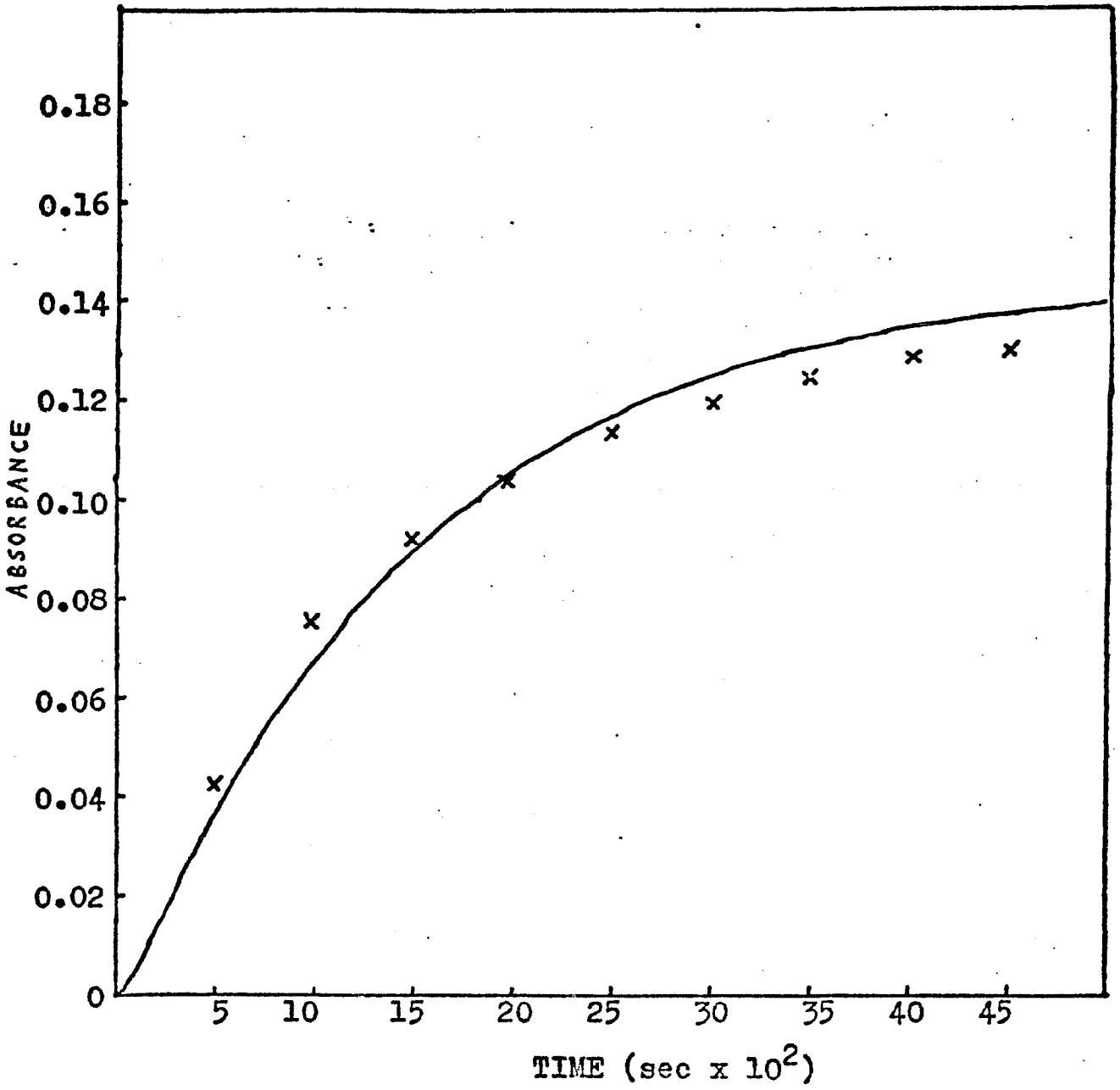

$[Cr]_T = 2.50 \times 10^{-3}$ M, $[H_2O_2] = 1.27 \times 10^{-3}$ M, k_3 = zero
Values for all other variables are given in Appendix (II-B), which contains the program for plotting the simulated kinetic trace. The crosses indicate experimental points.

Figure 16. Simulation of a Kinetic Trace.

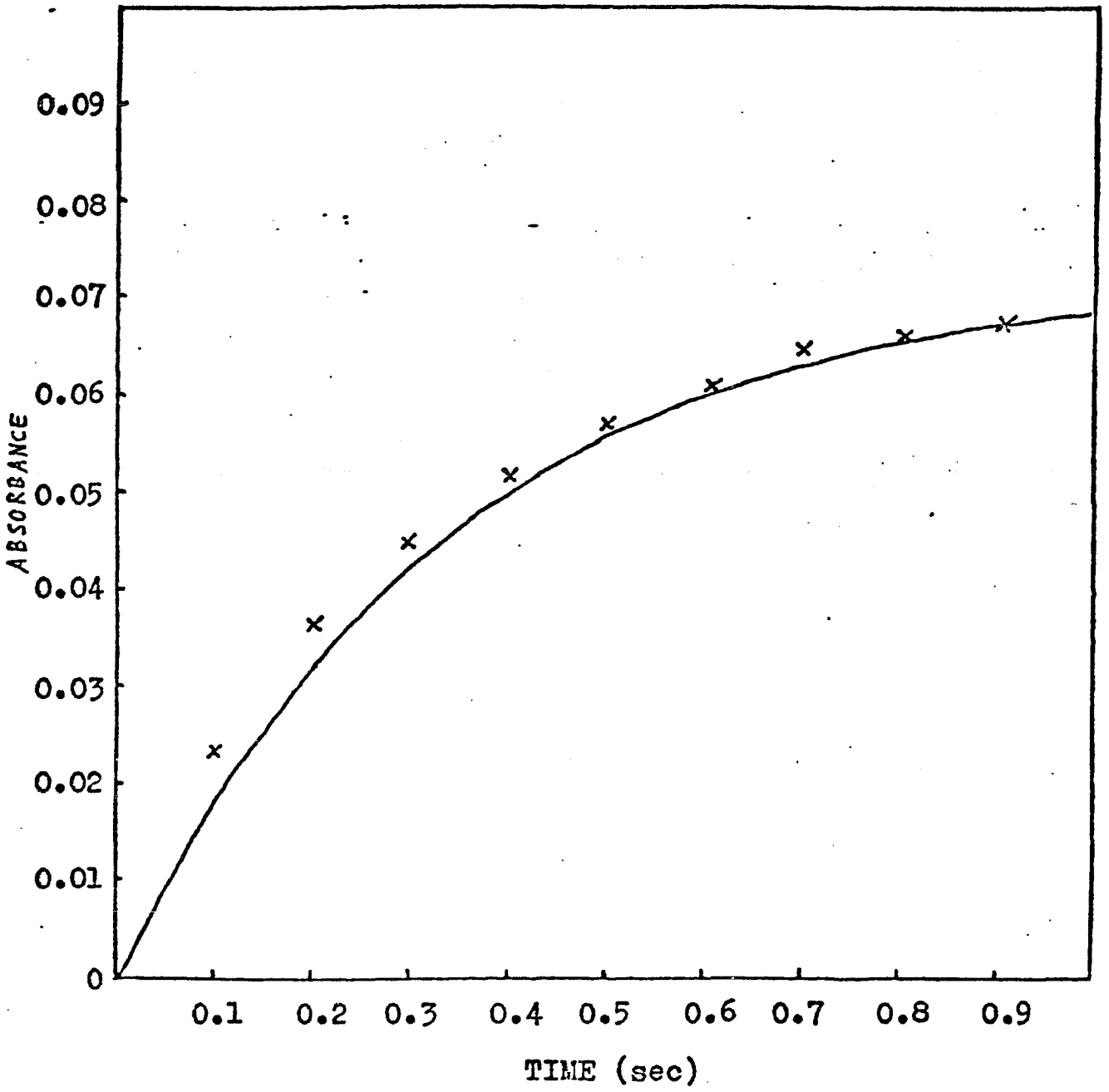

$[Cr]_T = 2.5 \times 10^{-3}$ M, $[H_2O_2] = 5.64 \times 10^{-4}$ M, k_3 = zero
Values for all other variables are given in Appendix (II-B), which contains the program for plotting the simulated kinetic trace. The crosses indicate experimental points.

Figure 17. Simulation of a Kinetic Trace.

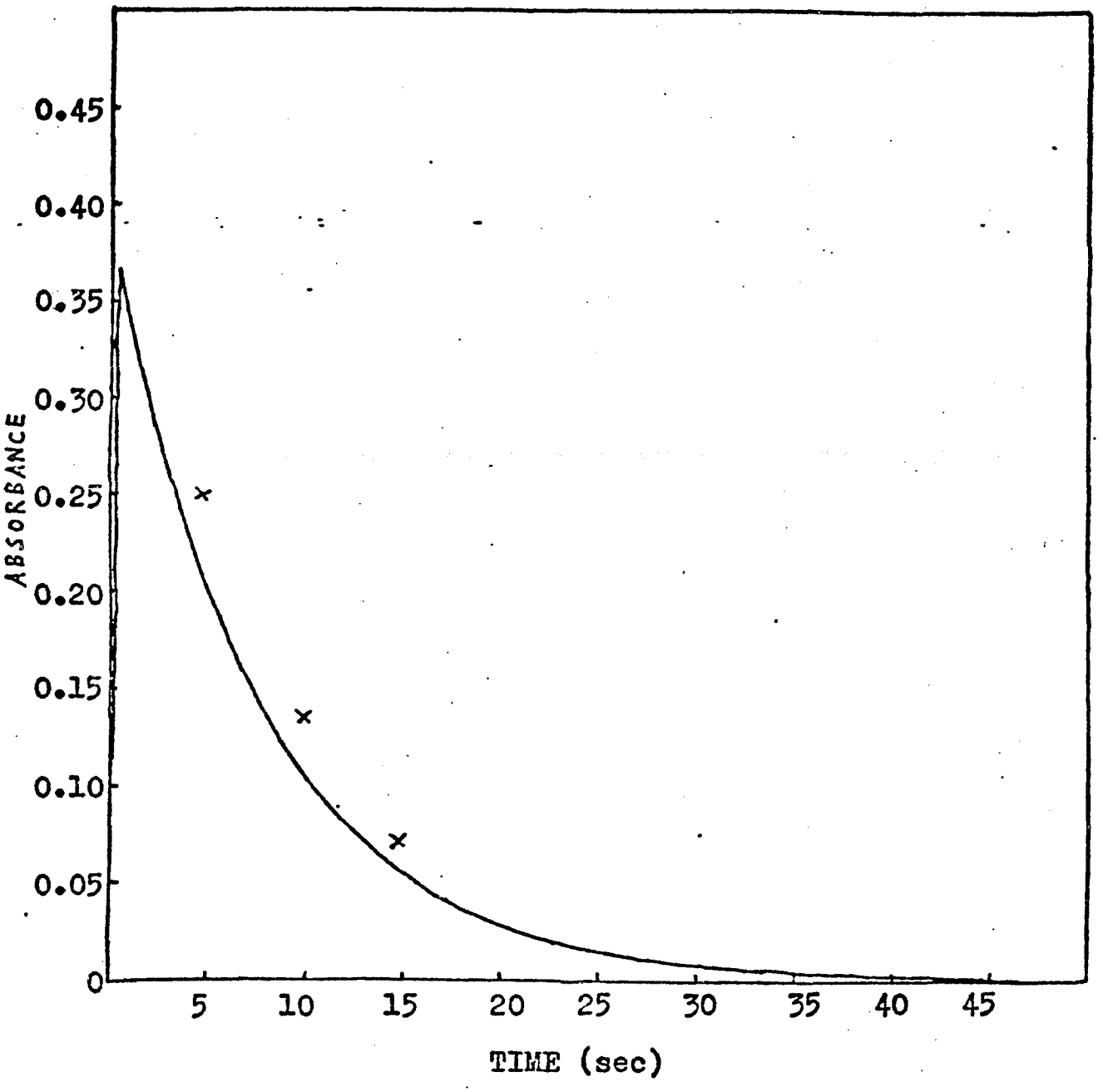

$[Cr]_T = 2.50 \times 10^{-3}$ M, $[H_2O_2] = 5.57 \times 10^{-3}$ M, $k_3 = 0.13$ sec^{-1}
Values for all other variables are given in Appendix (II-B), which contains the program for plotting the simulated kinetic trace. The crosses indicate experimental points.

Figure 18. Simulation of a Kinetic Trace.

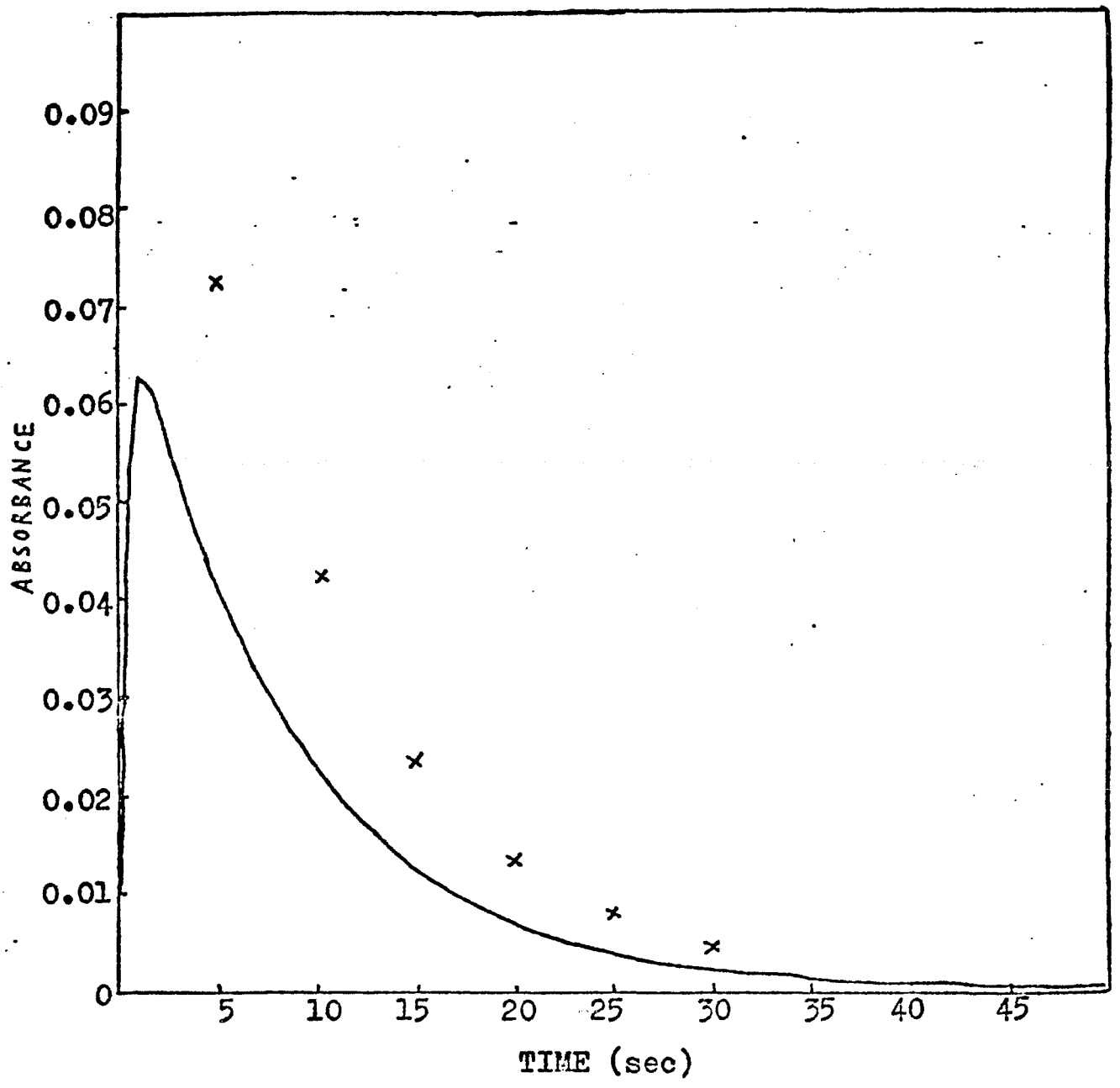

$[Cr]_T = 2.5 \times 10^{-3}$ M, $[H_2O_2] = 5.64 \times 10^{-4}$ M, $k_3 = 0.12$ sec^{-1}
Values for all other variables are given in Appendix (II-B), which contains the program for plotting the simulated kinetic trace. The crosses indicate experimental points.

Figure 19. Simulation of a Kinetic Trace.

to form a species C' with a similar absorptivity. This would account for the flatness of the peak at 500 nm. The species whose loss is represented by k_3 in Scheme III is thus C'. Consequently, the quantity [C] in eq. (56) and subsequent equations must be replaced by $[C_T]$ where $[C_T] = [C] + [C']$ and Scheme III must be modified to

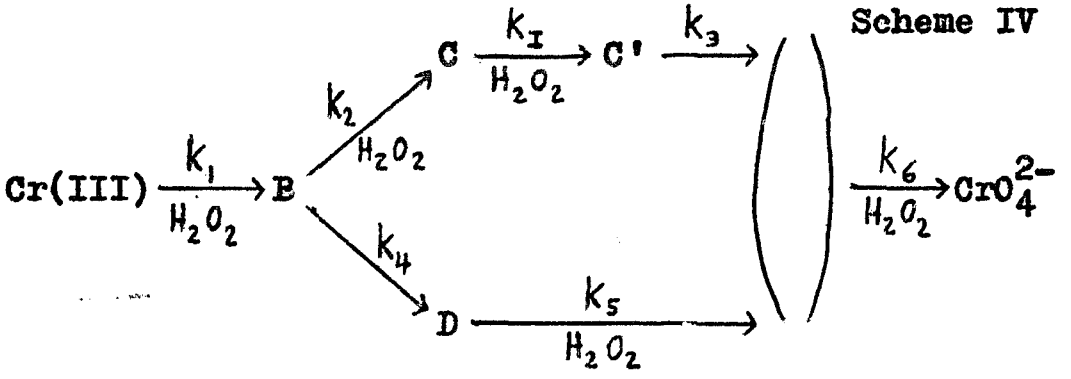

where k_I represents the rate constant for the induction period. The value of k_I cannot be determined.

It should be noted that there is a hydrogen peroxide dependency in the induction period as the extent of the displacement of the simulation from the actual kinetic is greater at lower hydrogen peroxide concentrations. Table (VIII) presents values for the rate constants shown in Scheme IV.

The plausibility of the values for k_2 and k_4, found through the technique of kinetic simulation, can be reinforced through the use of eq. (61). The successful use of k_1, k_2, and k_4 to predict values for $k_{obs}^{(1)}$ by means of this complicated relationship provides additional support for the mechanism. Figure (20) and Table (IX) show the compar-

TABLE VIII

RATE CONSTANTS FOR PROCESSES IN SCHEME IV

$k_1 = 5.3 \pm 1.0 \times 10^3\ M^{-1}\ sec^{-1}$

$k_2 = 2.0 \times 10^4\ M^{-1}\ sec^{-1}$

$k_3 = 0.11 \pm 0.02\ sec^{-1}$

$k_4 = 1.1 \times 10^2\ sec^{-1}$

$k_5 = 2.1 \pm 0.3 \times 10^2\ M^{-1}\ sec^{-1}$

$k_6 = 23 \pm 4\ M^{-1}\ sec^{-1}$

TABLE IX

COMPARISON OF EXPERIMENTAL AND CALCULATED VALUES FOR $k_{obs}^{(1)}$ AT 500 nm[a]

$[Cr]_T$ x 10^3	$[H_2O_2]$ x 10^4	$k_{obs}^{(1)}$ (sec^{-1})	$k_{obs}^{calc\ b}$ (sec^{-1})
1.00	3.16	1.5	1.6
1.00	5.53	3.2	2.8
1.00	9.86	6.6	4.9
1.00	12.5	7.7	6.2
1.00	23.9	11	11
1.50	4.49	2.0	2.3
1.50	8.08	4.1	4.1
2.50	5.64	3.8	2.9
2.50	12.7	8.1	6.3
2.50	12.9	7.7	6.4
2.50	15.1	7.7	7.4
2.50	34.2	16	16
2.50	34.8	17	16
2.50	39.4	17	18
2.50	55.7	25	25

a - Experimental values taken from Table (I).

b - The calculated k_{obs} is from eq. (61). Values for the rate constants used are: $k_1 = 5.3 \times 10^3\ M^{-1}\ sec^{-1}$ $k_2 = 2.0 \times 10^4\ M^{-1}\ sec^{-1}$, $k_4 = 1.1 \times 10^2\ sec^{-1}$

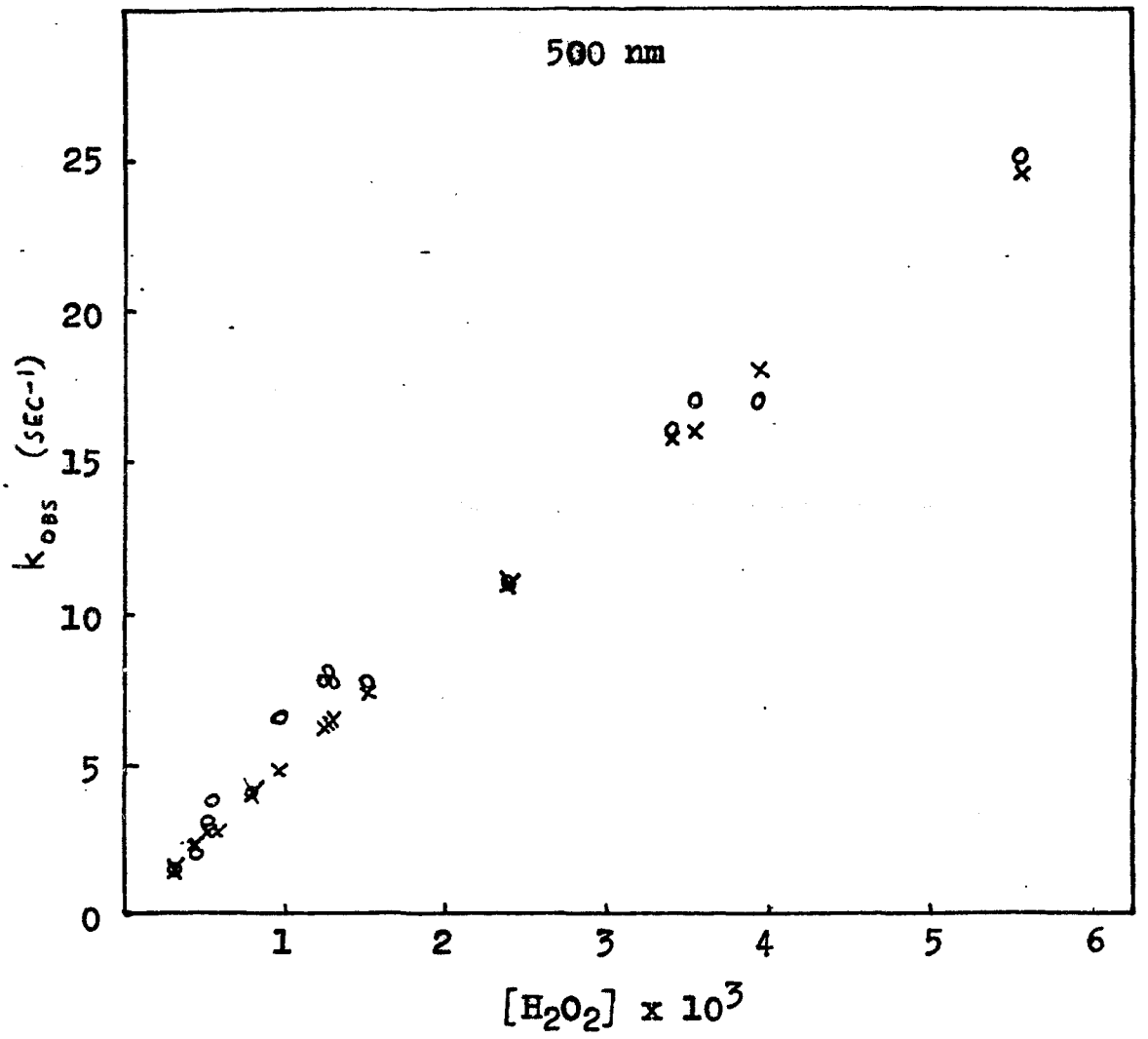

The circles and crosses represent experimental and calculated values, respectively.

This graph is based on the data in Table (IX).

Figure 20. Comparison of Experimental and Calculated Rate Constants.

ison between the experimental and calculated values. The agreement is excellent.

The losses of two species are being followed at 594 nm. The faster of the two processes being observed is that of the loss of D. The slower loss step is identical to that seen at 500 nm and, on that basis, must involve C'. Scheme IV does not show these intermediates going directly to product since the slow, hydrogen peroxide dependent absorbance increase at 374 nm continues long after C' and D have been consumed. Figure (21) shows the plot of k_{obs} vs. $[H_2O_2]$ for the slow step at 374 nm. The intercept is interpreted as due to an HO_2^- dependence.

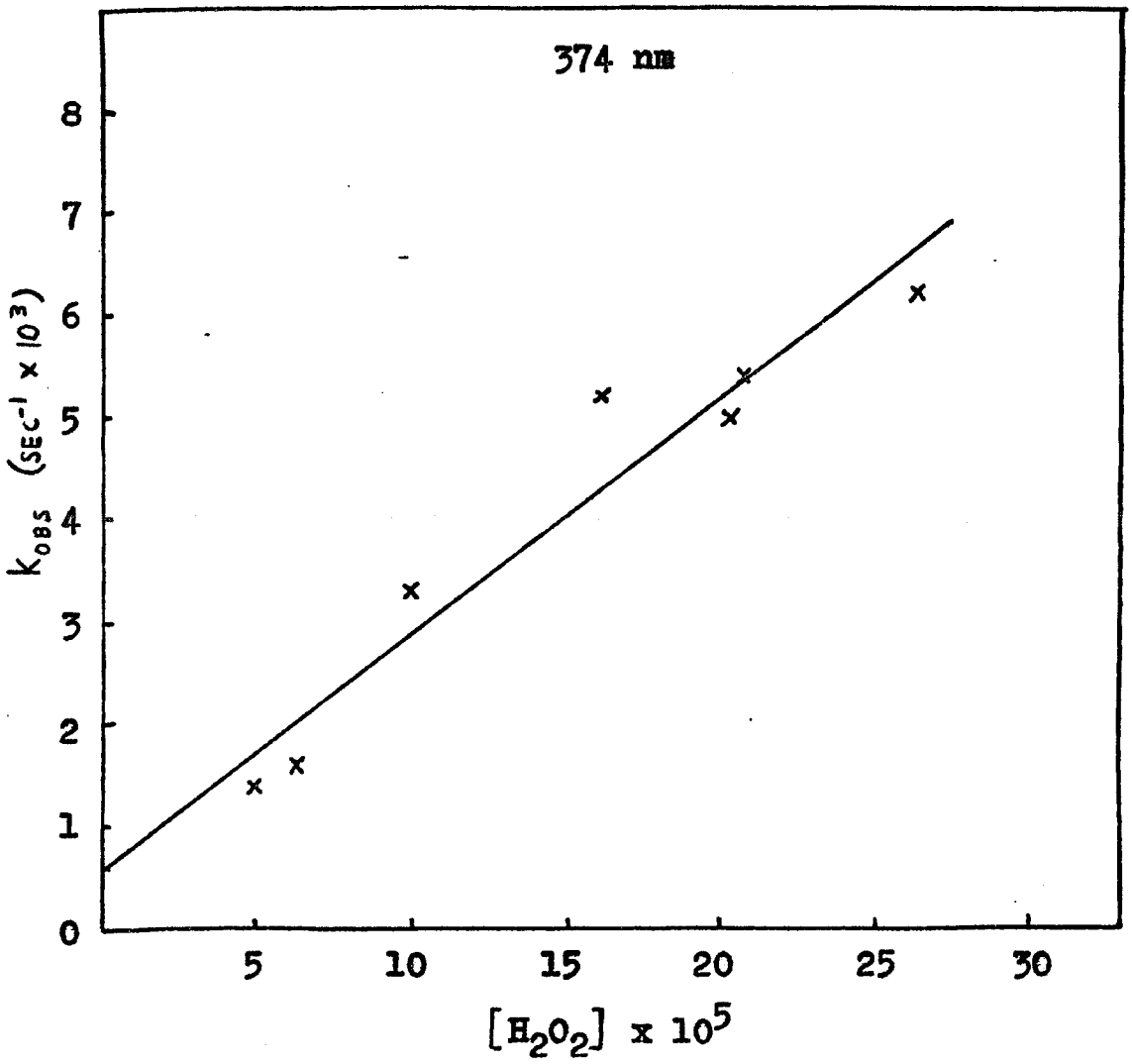

This graph is based on the data in Table (V).

The equation for the straight line, calculated by the method of least-squares, is

$$k_{obs} = 5.7 \times 10^{-4} + 23[H_2O_2] \quad .$$

Figure 21. Plot of k_{obs} vs. $[H_2O_2]$.
The slow reaction at 374 nm.

Discussion

The mathematics developed in the preceding sections has shown that the outline of the mechanism presented in Scheme IV is consistent with the experimental findings. Species corresponding to the letters which form a convenient shorthand for labelling the postulated intermediates remain to be assigned. The spectrophotometric evidence reveals a number of intermediates present but provides no means for identifying them. In the introduction to this work several studies were cited which suggest the presence of chromium(IV) and (V) species. As these species have unpaired electrons they should be accessible to investigation by esr spectroscopy.

An esr study of chromium(IV) in a solid at 4.2°K by Hoskins and Soffer[51] revealed a single absorption line with a linewidth exceeding 20 gauss. Increased temperature caused line broadening with consequent loss of signal well below liquid nitrogen temperature. To date, no one has ever succeeded in detecting an esr signal due to chromium(IV) in solution. Chromium(V), on the other hand, has been detected both in solid and in solution by means of esr. The first esr signal observed due to a chromium(V) species was studied by Carrington and coworkers.[52] The signal was due to CrO_4^{3-} and was found to be temperature dependent. The signal broadened and could no longer be observed above 20°K.

A detailed study of the esr spectra of various chromium(V) complexes in nonaqueous media was carried out by

Kon.[53] He found that for K_2CrOCl_5 in glacial acetic acid at room temperature the esr spectrum consisted of a single narrow peak (ΔH = 2.8 G) with a g value of 1.9877. Compounds of the type $CrORCl_4$ (where R = tetramethylammonium, pyridinium) were found to give narrow esr peaks with g values close to 1.988 whether dissolved in glacial acetic acid or in nitrobenzene.

The first esr study of a chromium(V) species produced as an intermediate during the course of a reaction was made by Wiberg and Schafer.[54] The system which was investigated by them was the oxidation of isopropyl alcohol by chromic acid in 97% acetic acid. The esr spectrum, consisting of a single well-defined peak with a g value of 1.9805, which they obtained was ascribed to a chromium(V) species. In addition, Wiberg and Schafer spectrophotometrically monitored an intermediate which absorbed at 510 nm and decayed at the same rate as the esr peak.

The experimental findings of the esr study carried out in the present work are quite similar to those reported by Wiberg and Schafer. The narrow peak observed in the chromium-hydrogen peroxide system has a g value of 1.977 and the rate of decay of the esr signal matches the rate of decay of the intermediate observed at 500 nm, the same spectral region in which Wiberg and Schafer recorded their spectrophotometric observations. For these reasons, chromium(V) is favored as the oxidation state of intermediates C and C'.

The possibility of species other than chromium(V) giving rise to an esr signal must now be considered. Although the balanced equation for the overall reaction [eq. (27)] does not indicate oxygen evolution, measurement of gas evolution during the course of a reaction revealed that the O_2:Cr(III) ratio exceeded 1:1 for $[Cr(III)]_T = 2.00 \times 10^{-3}$ M. The mechanism of oxygen evolution from alkaline hydrogen peroxide solutions proposed by Haber and Weiss[55] involves the production of hydroxyl and hydroperoxyl free radicals, both of which can be expected to give rise to esr signals. Another possible source of oxygen evolution is the decomposition of a chromium(VI)-hydrogen peroxide complex.

The possibility of the hydroperoxyl radical as the source of the observed esr signal can be immediately dispensed with. The esr peak due to $HO_2^{\bullet}$ has a linewidth of 27 G,[56] far wider than the peak observed here. The hydroxyl radical is also rejected as a possible source of the esr peak. The $OH^{\bullet}$ radical is very short-lived in basic media and esr spectra previously assigned to the species are now thought to be metal-hydroxyl radical complexes.[57,58] While a chromium-hydroxyl radical complex as the source of the sharp esr peak cannot be definitely ruled out, the similarity of the spectral data (visible and esr) for this system with that of the system of Wiberg and Schafer taken together with the observation that all previously reported metal-hydroxyl radical complexes have g values above 2.01 tends to strengthen the case for chromium(V) as the intermediate.[59,60]

The failure to detect hydroxyl and hydroperoxyl radicals may be due to their steady-state concentrations being too low to be monitored by esr.

A mechanism consistent with the experimental results is given below. In these reactions only the species of interest are shown.

$$Cr(III) + H_2O_2 \xrightarrow{k_1} Cr^{III}O_2 \qquad \text{formation of B} \qquad (74)$$

chromium(IV) pathway:

$$Cr^{III}O_2 \xrightarrow{k_4} Cr(IV) \qquad \text{formation of D} \qquad (75)$$

$$Cr(IV) + H_2O_2 \longrightarrow Cr^{IV}O_2 \quad \text{fast} \qquad (76)$$

$$Cr^{IV}O_2 + H_2O_2 \xrightarrow{k_5} Cr^{VI}O_2 \qquad (77)$$

(6 coordinate) (4 coordinate)

$$Cr^{VI}O_2 + H_2O_2 \xrightarrow{k_6} CrO_4^{2-} + O_2 \qquad (78)$$

chromium(V) pathway:

$$Cr^{III}O_2 + H_2O_2 \xrightarrow{k_2} Cr^{V}O_2 \qquad \text{formation of C} \qquad (79)$$

$$Cr^{V}O_2 + H_2O_2 \xrightarrow{k_I} Cr^{V}(O_2)_2 \qquad \text{formation of C'} \qquad (80)$$

$$Cr^{V}(O_2)_2 \xrightarrow{k_3} Cr^{VI}O_2 \qquad \text{loss of C'} \qquad (81)$$

(6 coordinate) (4 coordinate)

The rate constants k_1, k_2, k_3, k_4, k_5, k_6, and k_I are those assigned in Scheme IV. Equation (81) represents a combination of a change in coordination number followed by electron exchange. The change in coordination number is

rate determining.

A slow gain in absorbance was observed at 374 nm long after the loss of the esr signal and of the absorbing species at 500 and 594 nm. Therefore, chromium(IV) is shown [eq. (77)] going to a diamagnetic intermediate species, $Cr^{VI}O_2$, rather than to chromate (which is also diamagnetic). Chromium(V) is also shown going to a diamagnetic species [eq. (81)] since the second induction period at 500 nm appears to have a hydrogen peroxide dependency. The slow step at 374 nm is hydrogen peroxide dependent and suggests a peroxychromate species being lost by a reaction of the type presented in eq. (78). The slowness of the loss step (including the induction period) at 500 nm, represented by eqs. (80) and (81), may be due to a coordination change to the relatively more stable chromium(V) intermediate followed by its loss. The change in coordination as the "bottleneck" in the reduction of chromium(VI) to chromium(III) has been discussed in the introduction.

If the slow loss at 500 nm is due to a change in coordination number, the change must occur after chromium has reached the quinquevalent state since it is that state which is being detected by esr before the loss of intermediates C and C' begins. This raises the question as to why a coordination change should be slow once the quinquevalent state has been acheived. A possible answer lies in the fact that the ligands coordinated to a chromium(V) species will be predominantly covalently bound. Before the chromium(V) could

change from d^2sp^3 to sp^3 hybridization it would have to lose two ligands. This process can be thought of as being analogous to the rate determining step of an S_N1 substitution reaction, in which the bond strength of the dissociating ligand has a large influence on the rate because of the importance of bond breaking in that step. If the ligand-to-metal bond is strong, as would be the case for a covalently bound ligand, then the rate of ligand loss would be slow as would be the change of symmetry from six-coordinate to four-coordinate. Basolo and Pearson[61] present a good discussion of this effect. This could be resolved if the rate of ligand exchange to chromium(V) could be measured.

It was difficult to obtain kinetic data on the B $\longrightarrow$ D $\longrightarrow$( ) pathway because the step B $\longrightarrow$D could not be observed directly but was deduced through the mathematical treatment presented earlier. The fast loss D $\longrightarrow$( ) followed at 594 nm contributed only a small part to the total absorbance. Thus the hydrogen peroxide dependency and inverse hydroxide dependency of the step D $\longrightarrow$( ) was established but a precise value for k_5 could not be determined.

It should be noted that the kinetic evidence for the path B $\longrightarrow$C does not allow for the direct conversion of chromium(IV) to chromium(V). The peak at 500 nm, identified as due to a chromium(V) species from the esr data, is the result of either a two-electron change or oxygen atom transfer. Any contribution to the production of chromium(V) from the chromium(IV) of the other pathway in Scheme IV

would change the mathematics of eq. (69) which gave a linear plot. It follows from this that chromium(IV) must be consumed in a two-equivalent change.

APPENDIX I-A

Pseudo-Order Conditions

In all the reactions to be discussed, pseudo-order conditions have been established. This is a convenient kinetic technique for determining reaction orders.[62,63] For a given stoichiometry, one reactant is kept in limiting quantity with all other reagents in good excess (ten-fold or greater). During the course of a reaction, only the concentration of the material in limiting quantity changes appreciably while all other concentrations remain essentially fixed. It is thus the change in concentration of the limiting reactant with time that is being monitored. By way of illustration, for a system

$$A + B \xrightarrow{k_1} C + D$$

the rate law is

$$-d[A]/dt = k_1[A][B]$$

which is second order overall. However, if $[B] \gg [A]$ then the concentration of B is unchanged, to a good approximation. The result is that what is measured is

$$-d[A]/dt = k_{obs}[A]$$

which is first-order in A only. This is a pseudo-first-order reaction. The order of the reaction with respect to B is determined by varying B (while still keeping it in good excess over A) and observing the effect on k_{obs} ($= k_1[B]$).

APPENDIX I-B

Infinite-Time Method

When kinetic traces cannot be analyzed by the half-life method, often because of overlapping reactions, graphical methods must be employed.[64] Such is the case at 594 nm, where the fast loss step quickly becomes obscured by a slower loss process.

Assuming that Beer's law is obeyed, the absorbance due to a single species changes with time according to the relation

$$A_t = \epsilon l d_0 + \epsilon l d_1 e^{-m_1 t}$$

where ϵ is the absorptivity of the species being monitored, l is the optical path length, m_1 is the macroscopic rate constant, and d_0 and d_1 are constants representing concentrations of the species being monitored. At times large compared with $1/m_1$ the exponential term becomes insignificantly small with the result that

$$\lim_{t \to \infty} A_t = A_\infty = \epsilon l d_0$$

At 594 nm $A_\infty = 0$. Subtraction of this second equation from the first equation yields

$$A_t - A_\infty = \epsilon l d_1 e^{-m_1 t}$$

Taking logarithms gives

$$\ln|A_t - A_\infty| = \ln|\epsilon l d_1| - m_1 t$$

so that a plot of $\ln|A_t - A_\infty|$ vs. t gives a slope of $-m_1$.

APPENDIX I-C

Time-Lag Method

The time-lag method[65] is a graphical procedure for determining the value of a macroscopic rate constant. It is more convenient than the infinite-time method in that logarithms need only be taken once. In addition, the slope of the line is most strongly influenced by the earliest, most reliable data. The drawback of this method is that more experimental points are required than for the infinite-time method since they are evaluated in pairs.

Let the absorbance at time t, A_t, be given by

$$A_t = \epsilon l c_o + \epsilon l c_1 e^{-m_1 t}$$

and at time $t+\tau$ by

$$A_{t+\tau} = \epsilon l c_o + \epsilon l c_1 e^{-m_1 (t+\tau)}$$

Rearrangement and division of the first equation by the second yields

$$\frac{A_t - \epsilon l c_o}{A_{t+\tau} - \epsilon l c_o} = e^{m_1 \tau}$$

which further rearranges to give

$$A_t = \epsilon l c_o (1 - e^{m_1 \tau}) + A_{t+\tau}\ e^{m_1 \tau}$$

A plot of A_t vs. $A_{t+\tau}$ should give a straight line with a slope of $e^{m_1 \tau}$. Taking the logarithms of the slope and dividing by τ, the constant time interval between the pairs

plotted, results in a value for m_1, the macroscopic rate constant. This was the procedure employed at 374 nm.

APPENDIX II-A

Program for Calculating $[H_2O_2]$

Hydrogen peroxide exists predominantly as H_2O_2 and HO_2^- for the range of basicity of the present study. Since H_2O_2 appears to be the more reactive form, a calculation of its concentration is required for the analysis of the microscopic rate constants for the reactions in which it participates.

From the equilibrium expression

$$\underset{a-x}{HO_2^-} + H_2O \rightleftharpoons \underset{x}{H_2O_2} + \underset{b-a+x}{OH^-} \qquad K_h$$

where K_h ($= 4.44 \times 10^{-3}$) is the equilibrium constant,[46] $a = [H_2O_2]_T$ (the total hydrogen peroxide concentration), $b = [OH^-]_T$ (hydroxide concentration after correction for conversion of $Cr(H_2O)_6^{3+}$ to CrO_2^-), and $x = [H_2O_2]$ (the actual H_2O_2 concentration), the relationship

$$K_h = \frac{x(b - a + x)}{a - x}$$

is established. This yields a quadratic equation which, upon solving and rejecting the negative root, gives

$$[H_2O_2] = \tfrac{1}{2}\left\{-(b - a + K_h) + \left[(b - a + K_h)^2 + 4\,K_h a\right]^{\frac{1}{2}}\right\}.$$

The following program was developed for use in the Hewlett Packard 9810A Calculator to solve the above equation:

```
000 clear
001 stop*
002 X→( )
003  0
004  0
005  1
006 Y→( )
007  0
008  0
009  2
010  -
011  4
012  .
013  4
014  4
015  4
016 enter exp
017 change sign
018  3
019  +
020 X⇄Y
021  ↑
022 x²
023 Y→( )
024  A
025 roll ↑
026  ↑
027  4
028  x
029 ( )→X
030  0
031  0
032  1
033  x
034  ↓
035  +
036  ↓
037  x
038  ↑
039  A
040  -
041  2
042  ÷
043  ↓
044  ↑
045  ↑
046 ( )→X
047  0
048  0
049  1
050 X⇄Y
051  -
052 ( )→X
053  0
054  0
055  2
056 X⇄Y
057  -
058 end
```

* ENTER: Y register - $[OH^-]_T$

X register - $[H_2O_2]_T$

then press "continue".

To start: press - go to
end
continue

FINAL DISPLAY

Z register - $[H_2O_2]$

Y register - $[OH^-]_c$

X register - $[HO_2^-]$

APPENDIX II-B

Simulation of Kinetic Traces

The expression for the concentration of species C at any time

$$[C] = -\frac{k_1k_2[H_2O_2]^2[Cr(III)]_T\ e^{-k_1[H_2O_2]t}}{\{(k_2 - k_1)[H_2O_2] + k_4\}(k_1[H_2O_2] - k_3)}$$

$$+\frac{k_1k_2[H_2O_2]^2[Cr(III)]_T\ e^{-(k_2[H_2O_2] + k_4)t}}{\{(k_2 - k_1)[H_2O_2] + k_4\}(k_2[H_2O_2] + k_4 - k_3)}$$

$$+\frac{k_1k_2[H_2O_2]^2[Cr(III)]_T\ e^{-k_3t}}{(k_1[H_2O_2] - k_3)(k_2[H_2O_2] + k_4 - k_3)} \qquad (56)$$

derived on p. (63) is of value in testing the proposed mechanism.

In part III of the Mechanism section it was shown that k_1 could be determined experimentally along with the ratio $k_4:k_2$, but the actual values of k_4 and k_2 could not be deduced from experiment. By using a program which would plot the variation of the concentration of species C with time, and comparing simulated traces utilizing different values of k_2 (and hence k_4) with experimental kinetic traces, values could be assigned to these two rate constants.

The following program plots the change in concentration of species C with time:

```
000 clear
001 stop
002 ( )→X
003  0
004  0
005  1
006  ↑
007 ( )→X
008  0
009  0
010  5
011  x
012 Y→( )
013  A
014  ↑
015 ( )  X
016  0
017  0
018  2
019  x
020 Y→( )
021  B
022  ↓
023 X⇄Y
024  -
025 ( )→X
026  0
027  0
028  4
029  +
030 Y→( )
031  0
032  1
033  4
034  A
035  ↑
036 ( )→X
037  0
038  0
039  3
040  -
041 Y→( )
042  0
043  1
044  3
045  ↑
046  B
047 X⇄Y
048  -
049 ( )→X
050  0
051  0
052  4
053  +
054 Y→( )
055  0
056  1
057  5
058 ( )→X
059  0
060  1
061  4
062  x
063 ( )→X
064  0
065  1
066  3
067  x
068  ↓
069 1/x
070  ↑
071  A
072  x
073  B
074  x
075 ( )→X
076  0
077  1
078  0
079  x
080 ( )→X
081  0
082  1
083  1
084  x
085 Y→( )
086  0
087  2
088  0
089  A
090  ↑
091 ( )→X
092  0
093  0
094  6
095  x
096 X⇄Y
097 change sign
098 exp
099  ↑
100 ( )→X
101  0
102  1
103  5
104  x
105 X⇄Y
106 change sign
107 X→( )
108  0
109  1
110  6
111 ( )→X
112  0
113  1
114  5
115 X⇄Y
116 ( )→X
117  0
118  0
119  3
120  +
121  ↓
122 X⇄Y
123  x
124 X⇄Y
125 change sign
126 exp
127  ↑
128 ( )→X
129  0
130  1
131  3
132  x
133 Y→( )
134  0
135  1
136  7
137  ↓
138 ( )→X
139  0
140  0
141  3
142  x
143 X⇄Y
144 change sign
145 exp
146  ↑
147 ( )→X
148  0
149  1
```

```
150  4
151  x
152 Y→( )
153  0
154  1
155  8
156 ( )→X
157  0
158  1
159  7
160  +
161 ( )→X
162  0
163  1
164  6
165  +
166 Y→( )
167  0
168  1
169  9
170 ( )→X
171  0
172  2
173  0
174  x
175 ( )→X
176  0
177  0
178  9
179  ÷
180  9
181  9
182  9
183  9
184  x
185  ↑
186 ( )→X
187  0
188  0
189  6
190  x
191 ( )→X
192  0
193  0
194  8
195  ÷
196  ↓
197 FMT
198  ↓
199 ( )→X
200  0
201  0
202  6
203  ↑
204 ( )→X
205  0
206  0
207  7
208  +
209 Y→( )
210  0
211  0
212  6
213 ( )→X
214  0
215  0
216  8
217 IF X < Y
218  0
219  2
220  2
221  7
222 go to
223  0
224  0
225  8
226  9
227 end
```

The following variables must be entered into the indicated storage locations prior to running the program:

001 - k_1 005 - $[H_2O_2]$ 009 - $(O.D.)_{max}$

002 - k_2 006 - t 010 - ϵ

003 - k_3 007 - Δt 011 - $[Cr]_T$

004 - k_4 008 - t_{max}

The value of t entered into location 006 is that for the initial time, usually zero. Location 007 contains the value by which t is incremented and location 008 contains the maximum value of t. If ϵ of location 010 is set equal to one, then the variation of the concentration of species C with time is being plotted. Introduction of a value for

the absorptivity of species C into location 010 results in absorbance being plotted against time. Location 009 contains the value of either the maximum concentration or maximum absorbance, depending on which is being plotted.

The following values were used in all simulations:

$k_1 = 5.3 \times 10^3 \ M^{-1} \ sec^{-1}$

$k_2 = 2.0 \times 10^4 \ M^{-1} \ sec^{-1}$

$k_4 = 1.1 \times 10^2 \ sec^{-1}$

$\epsilon = 310$

Since the formation and loss steps are decoupled in this system, k_3 must be set equal to zero when plotting the formation step at relatively low hydrogen peroxide concentrations. If this is not done, low absorbance values will be obtained.

References

1. F. H. Westheimer, Chem. Rev., 45, 419 (1949).
2. J. H. Espenson, Accts. Chem. Rsch., 3, 347 (1970).
3. G. P. Haight, Jr., T. J. Huang, and B. Z. Shakhashiri, J. Inorg. Nucl. Chem., 33, 2169 (1971).
4. F. Hasan and J. Rocek, J. Amer. Chem. Soc., 94, 3181, 9073 (1972).
5. C. Benson, J. Phys. Chem., 7, 1 (1903).
6. R. Lang and J. Zwerina, Z. anorg. Chem., 170, 389 (1928).
7. C. Altman and E. L. King, J. Amer. Chem. Soc., 83, 2825 (1961).
8. M. Ardon and R. A. Plane, J. Amer. Chem. Soc., 81, 3197 (1959).
9. L. S. Hegedus and A. Haim, Inorg. Chem., 6, 664 (1967).
10. R. W. Kolaczkowski and R. A. Plane, Inorg. Chem., 3, 322 (1964).
11. J. Y. Tong and E. L. King, J. Amer. Chem. Soc., 82, 3805 (1960).
12. J. H. Espenson, Inorg. Chem., 8, 1554 (1969).
13. N. Sutin, Accts. Chem. Rsch., 1, 225 (1968).
14. C. Postmus and E. L. King, J. Phys. Chem., 59, 1208 (1955).
15. J. I. Morrow and J. Levy, J. Phys. Chem., 72, 885 (1968).
16. L. G. Sillen, Acta Chem. Scand., 8, 299, 318 (1954).
17. L. Pokras, J. Chem. Educ., 33, 152, 223, 282 (1956).
18. H. T. Hall and H. Eyring, J. Amer. Chem. Soc., 72, 782 (1950).
19. K. G. Poulsen, J. Bjerrum, and I. Poulsen, Acta Chem. Scand., 8, 921 (1954).
20. J. A. Laswick and R. A. Plane, J. Amer. Chem. Soc., 81, 3564 (1959).

21. M. R. Baloga and J. E. Earley, J. Amer. Chem. Soc., 83, 4906 (1961).

22. D. A. House and C. S. Garner, Inorg. Chem., 5, 840 (1966).

23. D. A. House, R. G. Hughes, and C. S. Garner, Inorg. Chem., 6, 1077 (1967).

24. A. C. Adams, J. R. Crook, F. Bockhoff, and E. L. King, J. Amer. Chem. Soc., 90, 5761 (1968).

25. D. F. Evans, J. Chem. Soc., 4013 (1957).

26. D. G. Tuck and R. M. Walters, J. Chem. Soc., 3404 (1964).

27. P. Moore, S. F. A. Kettle, and R. G. Wilkins, Inorg. Chem., 3, 466 (1966).

28. F. A. Cotton and G. Wilkinson, "Advanced Inorganic Chemistry", 2nd ed. Interscience, New York, 1966 p. 828.

29. J. P. Hunt and H. Taube, J. Chem. Phys., 19, 602 (1951).

30. E. Huss and W. Klemm, Z. anorg. Chem., 262, 25 (1950).

31. W. Klemm, Angew. Chem., 66, 468 (1954).

32. R. Scholder, Angew. Chem., 65, 240 (1953).

33. R. Scholder, Angew. Chem., 66, 461 (1954).

34. O. G. Holmes and D. S. McClure, J. Chem. Phys., 26, 1686 (1957).

35. J. C. Sheppard and A. C. Wahl, J. Amer. Chem. Soc., 79, 1020 (1957).

36. L. Gjersten and A. C. Wahl, J. Amer. Chem. Soc., 81, 1572 (1959).

37. R. E. Connick, J. Amer. Chem. Soc., 71, 1528 (1949).

38. J. C. Sullivan, D. Cohen, and J. C. Hindman, J. Amer. Chem. Soc., 76, 4275 (1954).

39. W. J. Blaedel and V. W. Meloche, "Elementary Quantitative Analysis" Harper & Row, New York, 1963 p. 795 .

40. J. I. Morrow, Chem. Instrum., 2, 375 (1970).

41. American Instrument Co., Inc., "Aminco-Morrow Stopped-Flow Apparatus", cat. no. 4-8409 instruction no. 939-A.

42. S. W. Benson, "The Foundations of Chemical Kinetics", McGraw-Hill, New York, 1960 pp. 525 - 528.

43. J. I. Morrow, R. A. Pinkowitz, and J. Laufer, Inorg. Chem., 5, 934 (1966).

44. J. E. Wertz and J. R. Bolton, "Electron Spin Resonance", McGraw-Hill, New York, 1972 p. 12 .

45. Ibid. p. 465 .

46. M. G. Evans and N. Uri, Trans. Faraday Soc., 45, 225 (1949).

47. G. Davies, N. Sutin, and K. O. Watkins, J. Amer. Chem. Soc., 92, 1892 (1970).

48. P. B. Chock, R. B. K. Dewar, J. Halpern, and L.-Y. Wong, J. Amer. Chem. Soc., 91, 82 (1969).

49. F. A. Matsen and J. L. Franklin, J. Amer. Chem. Soc., 72, 3337 (1950).

50. J.-Y. Chien, J. Amer. Chem. Soc., 70, 2256 (1948).

51. R. H. Hoskins and B. H. Soffer, Phys. Rev., 133, 490 (1964).

52. A. Carrington, D. J. E. Ingram, H. Schonland, and M. C. R. Symons, J. Chem. Soc., 4710 (1956).

53. H. Kon, J. Inorg. Nucl. Chem., 25, 933 (1963).

54. K. B. Wiberg and H. Schafer, J. Amer. Chem. Soc., 91, 927, 933 (1969).

55. F. Haber and J. Weiss, Proc. Royal Soc., A147, 332 (1934).

56. E. Saito and B. H. J. Bielski, J. Amer. Chem. Soc., 83, 4467 (1961).

57. Y. S. Chiang, J. Craddock, D. Mickewich, and J. Turkevich, J. Phys. Chem., 70, 3509 (1966).

58. A. Samuni, J. Phys. Chem., 76, 2207 (1972).

59. M. S. Bains, J. C. Arthur, Jr., and O. Hinojosa, Inorg. Chem., 9, 1571 (1970).

60. A. Samuni and G. Czapski, J. Phys. Chem., 74, 4592 (1970).

61. F. Basolo and R. G. Pearson, "Mechanisms of Inorganic Reactions", 2nd ed. Wiley, New York, 1967 pp. 137, 166.

62. R. G. Wilkins, "The Study of Kinetics and Mechanism of Reactions of Transition Metal Complexes", Allyn and Bacon, Boston, 1974 pp. 8 - 15 .

63. S. W. Benson, Op. Cit., p. 81 .

64. G. M. Fleck, "Chemical Reaction Mechanisms", Holt, Rinehart and Winston, New York, 1971 p. 36 .

65. Ibid., p. 41 .